FIGURE 1-1
VIKING ORBITER PICTURE FORMAT

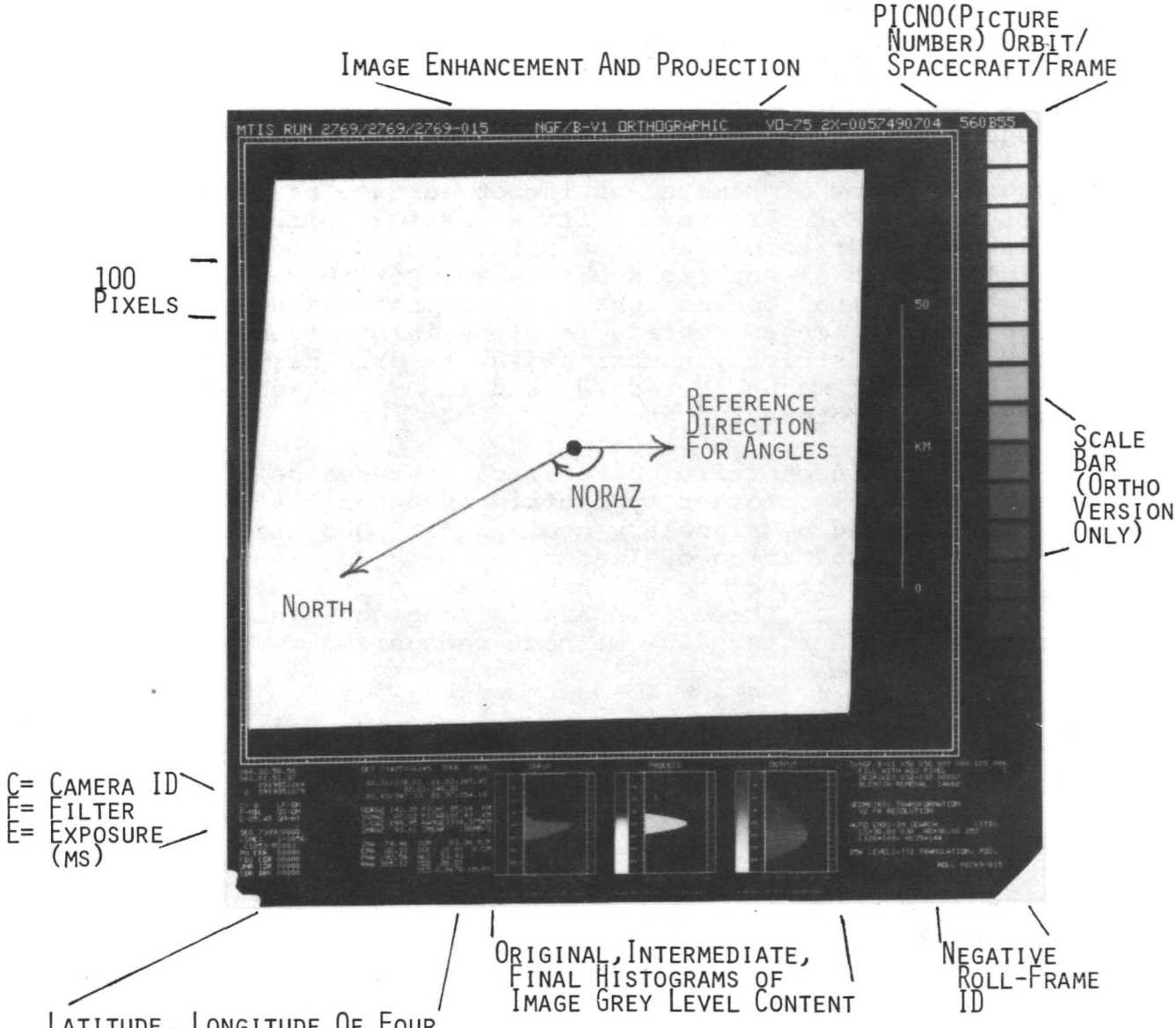

NORAZ= AZIMUTH OF NORTH (SEE EXAMPLE)
SUNAZ= AZIMUTH OF SUB-SOLAR POINT
S/CAZ= AZIMUTH OF SUB-SPACECRAFT POINT
SMRAZ= SMEAR AZIMUTH
INA= SUN ZENITH ANGLE
EMA= S/C ZENITH ANGLE
PHA= SOLAR PHASE ANGLE
RHA= HOUR ANGLE (DEG)

PICHT= FRAME HEIGHT
PICWD= FRAME WIDTH
RANGE= S/C TO FRAME CENTER DISTANCE
SMEAR= SMEAR RATE(IMAGE PLANE)
SCM= IMAGE SCALE(M/PIXEL) SCR VERSION
SCK= IMAGE SCALE(KM/CM) CONTACT PRINT
ALS= AEROCENTRIC LONGITUDE SUN (MARTIAN SEASON)
TOD= TIME OF DAY (HRS)

SCO= IMAGE SCALE(M/PIXEL) ORTHO VERSION

SURFACE ACOUSTIC WAVE STABILIZED OSCILLATORS

(NASA-CR-159980) SURFACE ACOUSTIC WAVE STABILIZED OSCILLATORS Final Report, 15 Aug. 1978 - 14 Aug. 1979 (Raytheon Co.)
79 p HC A05/MF A01 CSCL 09A

N80-24552

Unclas
G3/33 22050

RAYTHEON RESEARCH DIVISION
28 SEYON STREET
WALTHAM, MASSACHUSETTS 02154

SEPTEMBER 15, 1979

FINAL REPORT FOR NAS5-25117

PREPARED FOR:

GODDARD SPACE FLIGHT CENTER
GREENBELT, MARYLAND 20771

1. Report No.	2. Government Accession No.	3. Recipient's Catalog No.
4. Title and Subtitle Surface Acoustic Wave Stabilized Oscillators		5. Report Date September 1979 6. Performing Organization Code S-2604
7. Author(s) T.E. Parker, D.L. Lee, and I. Leja		8. Performing Organization Report No.
9. Performing Organization Name and Address Raytheon Research Division 28 Seyon Street Waltham, Massachusetts 02154		10. Work Unit No. 11. Contract or Grant No. NAS5-25117
12. Sponsoring Agency Name and Address National Aeronautics & Space Administration Goddard Space Flight Center Greenbelt Road Greenbelt, Maryland 20771		13. Type of Report and Period Covered Final Report Aug 1978 - Aug 1979 14. Sponsoring Agency Code
15. Supplementary Notes		

16. Abstract

Four areas of surface acoustic wave (SAW) controlled oscillators were investigated and a number of 401.2 MHz oscillators were constructed that showed improved performance. Aging studies on SAW devices packaged in HC36/U cold weld enclosures produced frequency drifts as low as 0.4 ppm in 35 weeks and drift rates well under 0.5 ppm/year. Temperature compensation circuits have substantially improved oscillator temperature stability, with a deviation of ±4 ppm observed over the range -45°C to +40°C. High efficiency amplifiers have been constructed for SAW oscillators and a dc to rf efficiency of 44 percent has been obtained for an rf output power of 25 mW. Shock and vibration tests were made on four oscillators and all survived 500 G shock pulses unchanged. Only when white noise vibration (20 Hz to 2000 Hz) levels of 20 G's rms were applied did some of the devices fail.

17. Key Words (Selected by Author(s))	18. Distribution Statement
Oscillator Aging Surface Acoustic Wave Temperature Compensation High Efficiency	

19. Security Classif. (of this report)	20. Security Classif. (of this page)	21. No. of Pages	22. Price*
Unclassified	Unclassified	77	

SURFACE ACOUSTIC WAVE STABILIZED OSCILLATORS

Raytheon Research Division
28 Seyon Street
Waltham, Massachusetts 02154

September 15, 1979

Final Report for NAS5-25117

Prepared for:

Goddard Space Flight Center
Greenbelt, Maryland 20771

TABLE OF CONTENTS

		Page
	LIST OF ILLUSTRATIONS	v
	LIST OF TABLES	vii
1.0	INTRODUCTION	1-1
	1.1 Overall Goals	1-1
	1.2 Specific Device Goals	1-2
	1.2.1 Output frequency	1-2
	1.2.2 Output frequency stability	1-2
	1.2.3 Device output level	1-2
	1.2.4 Device dc power source	1-2
	1.2.5 Temperature environment	1-3
	1.2.6 Shock and vibration	1-3
	1.3 Problem Areas	1-4
	1.4 Tasks Performed	1-4
2.0	EXECUTIVE SUMMARY	2-1
	2.1 Task I	2-1
	2.2 Task II	2-1
	2.3 Task III	2-2
	2.4 Task IV	2-2
3.0	TASK I - AGING	3-1
	3.1 Device Fabrication and Sealing	3-1
	3.2 Device Tests and Short-Term Frequency Stability	3-4
	3.3 Aging Data	3-7
	3.4 Analysis of Aging Data	3-7
	3.5 Mathematical Modeling of the Aging Data	3-17
	3.6 Conclusions	3-26
4.0	TASK II - TEMPERATURE COMPENSATION	4-1
	4.1 Oscillator Configuration	4-1
	4.2 Delay Line Temperature Characteristics	4-1

TABLE OF CONTENTS (Continued)

		Page
4.3	Passive Compensation Techniques	4-3
4.4	Active Compensation Technique	4-6
4.5	Sources of Compensation Error	4-9
4.6	Conclusions	4-12
5.0	TASK III - HIGH EFFICIENCY AMPLIFIER	5-1
5.1	Introduction	5-1
5.2	GaAs FET (Raytheon LND-832) Oscillator	5-3
5.3	Silicon FET (Signetics SO-303) Oscillator	5-9
5.4	Conclusions	5-11
6.0	TASK IV - SHOCK AND VIBRATION TESTS	6-1
6.1	Specified Tests	6-1
6.2	Test Devices	6-1
6.3	Results of Tests	6-1
6.4	Conclusions	6-5
7.0	CONCLUSIONS	7-1

LIST OF ILLUSTRATIONS

Number		Page
3.1	SAW Delay Line Mounted in HC36/U Package	3-3
3.2	Circuit for a SAW Controlled Oscillator	3-6
3.3	Aging Data for SAW Devices, with Aluminum Transducers, Sealed in HC36/U Enclosures	3-8
3.4	Aging Data for SAW Devices, with Gold Transducers, Sealed in HC36/U Enclosures	3-9
3.5	Aging Data for SAW Devices, with Aluminum Transducers, Sealed in Flatpacks	3-10
3.6	Aging Data for SAW Devices, with Gold Transducers, Sealed in Flatpacks	3-11
3.7	Aging Data for SAW Devices with Package Leaks	3-13
3.8	Frequency Drift in First Ten Weeks as a Function of the Time from Transducer Fabrication to Start of the Aging Test, T_{fs}	3-15
3.9	Log Fit to Aging Data	3-20
3.10	Log Fit to Aging Data	3-21
3.11	Log Fit to Aging Data	3-22
3.12	Log Fit to Aging Data	3-23
3.13	Log Fit to Aging Data	3-24
4.1	SAW Delay Line Oscillator with Electronic Temperature Compensation	4-2
4.2	Passive Compensation Circuit	4-4
4.3	Phase-Lock Circuitry Used to Determine Control Voltage for Fixed Frequency	4-5
4.4	Comparison Between Uncompensated and Compensated Response Using Passive Compensation Circuit	4-7
4.5	Low Power Active Compensation Circuit	4-8
4.6	Comparison Between Uncompensated and Compensated Response Using Active Compensation Circuit	4-10

LIST OF ILLUSTRATIONS (Continued)

Number		Page
4.7	Phase Shifter Induced Thermal Hysteresis	4-11
4.8	Measured Temperature Dependence of Phase Shift for High Gain rf Amplifiers	4-13
5.1	Schematic of Oscillator using LND 832 Dual-Gate FET	5-4
5.2	Dependence of GaAs FET Oscillator Frequency on Drain Voltage, V_{dd}, for Several Values of Gate Voltage, V_g	5-8
5.3	Schematic of Oscillator Using SD 303 Dual-Gate FET	5-10
5.4	Dependence of Silicon FET Oscillator Frequency on Voltage from dc Power Supply	5-12
6.1	SAW Device Mounted in a Flatpack	6-2
6.2	Illustration of Mounting Technique Using Spring Clips and Polyimide Adhesive	6-3

LIST OF TABLES

Number	Title	Page
3-1	List of Devices in Aging Tests	3-12
5-1	Reactive Loading of Various Circuit Elements	5-5

1.0 INTRODUCTION

One of the more promising uses for surface acoustic wave (SAW) devices is as a controlling element for oscillators. The SAW controlled oscillator is a very simple device consisting of a SAW delay line (or resonator) and an amplifier with sufficient gain to overcome the loss in the SAW device. The great advantage of the SAW oscillator is that very high frequency operation is readily achievable, while at the same time the high stability of a quartz crystal is maintained.

SAW oscillators operating above 1 GHz have been demonstrated and can greatly reduce the complexity of high frequency sources by eliminating many stages of multiplication. This can also reduce the size, power consumption, and cost of these sources. Furthermore, reducing the multiplication significantly reduces the FM noise of a high-frequency source.

An additional advantage of SAW-controlled oscillators is the great design flexibility inherent in SAW devices. Delay lines provide a wide tuning range, linear phase, and multifrequency cpability. SAW resonators (the surface wave equivalent of the quartz crystal resonators) provide high Q and the lowest noise.

1.1 Overall Goals

The overall goal of this program was to identify the problems present in SAW oscillators and to develop the necessary technology to solve them. An integral part of this goal is the production and testing of a number of SAW oscillators. Through the evaluation of these oscillators, the optimum choice of materials and procedures can be made.

This report covers the second part of a program that started in September, 1976. During the first part, photomasks were designed for a 401.2 MHz oscillator using three different fabrication techniques. These included aluminum and gold transducers on ST-cut quartz and aluminum transducers on

the $SiO_2/LiTaO_3$ structure. Devices using all three approaches were fabricated and their performance was evaluated. The results of these evaluations were presented in NASA Final Report NAS5-23701.[1.1]

1.2 Specific Device Goals

To help evaluate the performance of SAW oscillators, operating requirements reflecting real system specifications were chosen as specific device goals. These requirements are listed below.

1.2.1 Output frequency

The output frequency of the device shall be 401.2 MHz ± 6.0 KHz.

1.2.2 Output frequency stability

The short term frequency stability in any one second shall be at least 1×10^{-9} in the environment in which the package must operate. The total frequency change in any fifteen (15) minutes shall not exceed 4.2 Hz. The rate of the frequency change shall not exceed 0.28 Hz per minute.

1.2.3 Device output level

When operated from a voltage source whose terminal voltage, underload, is 12.0 volts, +2 volts, -4 volts the output of the device shall not drop below a level of 13.9 dBm (25 milliwatts) in the environment in which the unit must operate.

1.2.4 Device dc power source

The dc power source for the device shall be a battery pack. A fully charged battery pack can be expected to have a terminal voltage, underload, of 14.0 volts. The battery pack shall be considered unusable when the underload terminal voltage has been reduced to 8.0 volts.

1.2.5 Temperature environment

The operating temperature environment shall be over a range of -40°C to +45°C. The storage temperature environment shall be over a range of -55°C to +80°C. The maximum rate of temperature change shall be 3°C/min.

1.2.6 Shock and vibration

1.2.6.1 Shock

SAW oscillator devices shall be tested in accordance with method 213 of MIL-STD-202. The following details shall apply:

(a) Test Condition - I (100G)

(b) Measurement required before and after test - Frequency, short term stability, and etc.

NOTE: *There must be no deviation of the after test measurements from the before test measurements.*

1.2.6.2 Vibration

SAW oscillator devices shall be tested in accordance with method 201 in MIL STD-202. The following details shall apply:

(a) Test Condition (as specified)

(b) Measurements required before and after test - Frequency, short term disability, and etc.

NOTE: *There must be no deviation of the after test measurements from the before test measurements.*

1.3 Problem Areas

From our experience with the oscillators constructed in the first part of the program, it is clear that some of these requirements are readily met. Others, however, are much more difficult to achieve. Operation at 401.2 MHz was readily accomplished and a short-term stability of better than 1×10^{-9} was demonstrated. Furthermore, it was determined that a power output level of 25 milliwatts was reasonable. However, some areas where further improvement was required became apparent. The long-term frequency drift of the SAW oscillators constructed during the first phase was observed to range from 2.5 to 16 ppm in the first six months. This was not considered adequate, since aging would use up nearly all ofthe ±6 KHz window and leave no flexibility for other parameters.

Another problem area identified was temperature stability. The inherent material stability of rotated Y cut quartz is ±37 ppm (±15 KHz), in the range -40 to +45°C. This does not meet the requirement of a ±6 KHz window, and it also makes the requirement of 4.2 Hz drift in 15 minutes extremely difficult to meet. Clearly some improvement was required.

A third area where improved performance was also required was dc to rf efficiency. With commercially available linear, wideband amplifiers, the best that can be achieved (at low power levels) is about 3 percent. This is clearly not satisfactory for battery operation, where power consumptions must be minimized.

1.4 Tasks Performed

To solve the problems discussed above and to evaluate sensitivity to shock and vibration, four distinct tasks were accomplished during the course of the program. The first was to evaluate cold weld enclosures for low aging by having ten devices sealed at the U. S. Army Electronics Research and Development Command (ERADCOM) in Ft. Monmouth, New Jersey. The aging data from those devices and all earlier devices was evaluated and analyzed. Package leaks and the SAW transducer metallization were identified as probable

sources of frequency drift. Procedures to further reduce aging are suggested in this report. Also included in this task were measurements on the sealed devices to determine the frequency distribution of the SAW devices.

The second task was the development of temperature compensation circuits to improve the temperature stability of the SAW oscillators. Low-power active and passive circuits were both investigated. An improvement in temperature stability of more than a factor of ten was achieved.

The third task was the development of a high-efficiency amplifier to minimize the power consumption of the oscillator. One amplifier using a dual-gate silicon FET and two using dual-gate GaAs FET's were built. Overall dc to rf efficiencies as high as 44 percent were achieved.

The fourth and final task was to perform the shock and vibration tests as specified in Sec. 1.2. The required tests were performed and the levels were then increased until 2 of 4 oscillators malfunctioned.

REFERENCES

1.1 T. E. Parker, "Surface Acoustic Wave Stabilized Oscillators," Final Report NAS5-23701, September 1976 to December 1976, Raytheon Research Division, Waltham, Massachusetts, Jan. 1978.

2.0 EXECUTIVE SUMMARY

The objective of this program was to improve the performance of SAW controlled oscillators through the investigation of several problem areas. To accomplish this goal, four tasks were undertaken. The results from these four tasks are summarized below.

2.1 Task I

In order to evaluate cold weld packages for low aging, seven SAW delay lines were sealed and tested. The observed aging for these devices ranged from under 1 ppm to 5 ppm in 35 weeks. These results are considerably better than those for devices sealed in brazed flatpacks. One aging mechanism that was identified by this study is the downward drift caused by a package leak. The flatpacks showed this problem, but the cold weld packages have not. Analysis of the aging data has also shown that the relaxation process which causes most of the observed frequency drift starts at or near the time of transducer fabrication. The aging data fits well to a logarithmic model, and a very likely candidate for the physical mechanism is the relaxation of internal stress in the metal film of the transducer.

Preaging at 100°C for 10 days has resulted in a complex aging pattern but no significant reduction in the magnitude of the drift. However, preaging at 200°C has resulted in a frequency drift of only 0.4 ppm in 35 weeks. An rms frequency distribution of ±57 KHz was observed for the sealed SAW devices, with short term stability of 1.4×10^{-9}.

2.2 Task II

Active and passive temperature compensation circuits were constructed to give improved temperature stability. The passive circuit reduced the frequency deviation to ± 8 ppm for the range -45°C to +40°C. The active circuit gave better results with a deviation of ± 4 ppm for the same temperature range. Both circuits drew less than 1 mW of power. Some of the

oscillator characteristics that serve to limit the minimum frequency deviation were identified as temperature sensitive phase shifts in the amplifiers and electronic phase shifter.

With the improved temperature stability from the compensation circuits, the desired frequency stability of 4.2 Hz in 15 minutes can be reasonably approached through the design of a properly insulated enclosure for the oscillator.

2.3 Task III

The use of SAW oscillators in battery powered applications requires the development of high frequency, high efficiency amplifiers in order to minimize power consumption. Toward this goal three oscillators were constructed using dual gate FET amplifiers operated in a highly nonlinear switching mode. The best electrical performance was obtained with a design using a high frequency GaAs dual gate FET. This oscillator delivered in excess of 25 mW of rf power with a dc to rf efficiency of 44 percent. However, the voltage dependence of the gate capacitance on the GaAs FET resulted in relatively poor frequency stability.

Better frequency stability was obtained with a design using a silicon dual gate FET, but the electrical performance was not as good. This oscillator delivered 20 mW of rf with an efficiency of 9 percent. The frequency stability, however, was essentially as good as that obtained with commercial wideband amplifiers.

2.4 Task IV

Shock and vibration tests were performed in order to test the ability of SAW devices to withstand the affects of acceleration. Four oscillators were subjected to shock pulses of up to 500 G's with no observable change before and after the tests. In addition, no change was observed for vibration from 10 to 55 Hz through a 0.03-in. displacement, or for white noise from 20 to 2000 Hz at an rms level of 10 G's. Only when the level of the white noise

was increased to 20 G's did two of the devices fail. One failure was traced to a loose electrical connection, while the other problem proved to be intermittent and disappeared before it could be identified.

3.0 TASK I - AGING

Cold weld enclosures have proven to be a good technique for achieving low aging in bulk wave quartz crystal resonators. Therefore, in light of the fact that the aging of SAW delay lines sealed in brazed flatpacks during the first part of the program proved to be too large, it was felt that the aging of SAW delay lines sealed in cold weld packages should be evaluated. To accomplish this, ten SAW delay lines were fabricated and sealed in HC36/U cold weld enclosures (only seven survived final testing and were put into testing). As a subsidiary part of this task, the frequency distribution of the sealed devices was determined in order to provide some data on the reproducibility of SAW delay lines.

3.1 Device Fabrication and Sealing

A total of ten SAW delay lines were prepared for sealing. These consisted of 6 devices with aluminum (Al) transducers on ST-cut quartz (40° rotated Y cut), 3 devices with gold (Au) transducers on ST-cut quartz, and one device with aluminum transducers on the SiO2/Y $LiTaO_3$ composite structure. The photomasks for the 401.2 MHz devices that were designed in the first half of this program were used for the fabrication of the present devices. Standard photolithographic techniques were used. The devices with aluminum transducers were fabricated with a 1000 Å metallization that was recessed into the quartz so that the top surface of the aluminum was level with the quartz surface. This was done to reduce spurious surface wave reflections caused by topographic discontinuities. The recessing was accomplished by first ion etching a 1000 Å deep pattern in the quartz, and then evaporating aluminum into the etched pattern.

The devices with gold transducers were fabricated with a 500 Å metallization. Because of the large disparity of surface wave velocities on gold and quartz, recessing was not used. In this case, the thinner metallization was used to keep reflections down to an acceptable level. Both the gold and aluminum devices were fabricated on "premium swept Q" quartz, which is the highest grade of synthetic quartz.

The one $SiO_2/LiTaO_3$ device that was prepared for sealing was fabricated during the first half of this program and had not been used at that time. Therefore it was available for use in this task.

The insertion loss of the various devices ranged from 17 dB for the $SiO_2/LiTaO_3$ device to 25 dB for the gold devices. The typical delay time, τ, was 1.6 μsec.

Figure 3.1 shows how the SAW delay lines were mounted in the HC36/U enclosure. A 0.010 in. stainless steel backing plate was spot welded to the base and a 0.007 in. stainless steel coil spring was then spot welded to the backing plate. The SAW substrates were then inserted into the spring clamp and the electrical connections were made with 0.002 in. gold wire. It should be noted here that the HC36/U is not an ideal package for SAW devices since it is somewhat larger than necessary and is not well suited for high frequency applications. However, facilities for sealing these packages were made available for this program, and the package was perfectly suitable for aging studies.

Since the packages were to be sealed at the U. S. Army Electronics Research and Development Command (ERADCOM) in Ft. Monmouth, New Jersey, a special machined aluminum container was made to transport the devices. Before mounting on the package base, the aluminum delay lines were rinsed in trichloroethylene and propanol and then blown dry. The gold devices were not rinsed because of the very fragile nature of the gold transducers. The bases and covers were separately rinsed, blown dry, and baked at 300°C. After the SAW devices were mounted, each was checked for electrical performance and then stored in a dry nitrogen atmosphere. Just before being transported to Ft. Monmouth, all of the devices were U.V.-cleaned for twenty minutes, then immediately placed in the transporting container, which was flushed with dry nitrogen and sealed.

The package sealing was performed at ERADCOM through the generous cooperation of John Vig, Ted Lukazek, and Ray Filler. Prior to sealing, the devices were given a final U.V. cleaning of 10 minutes and then were baked at

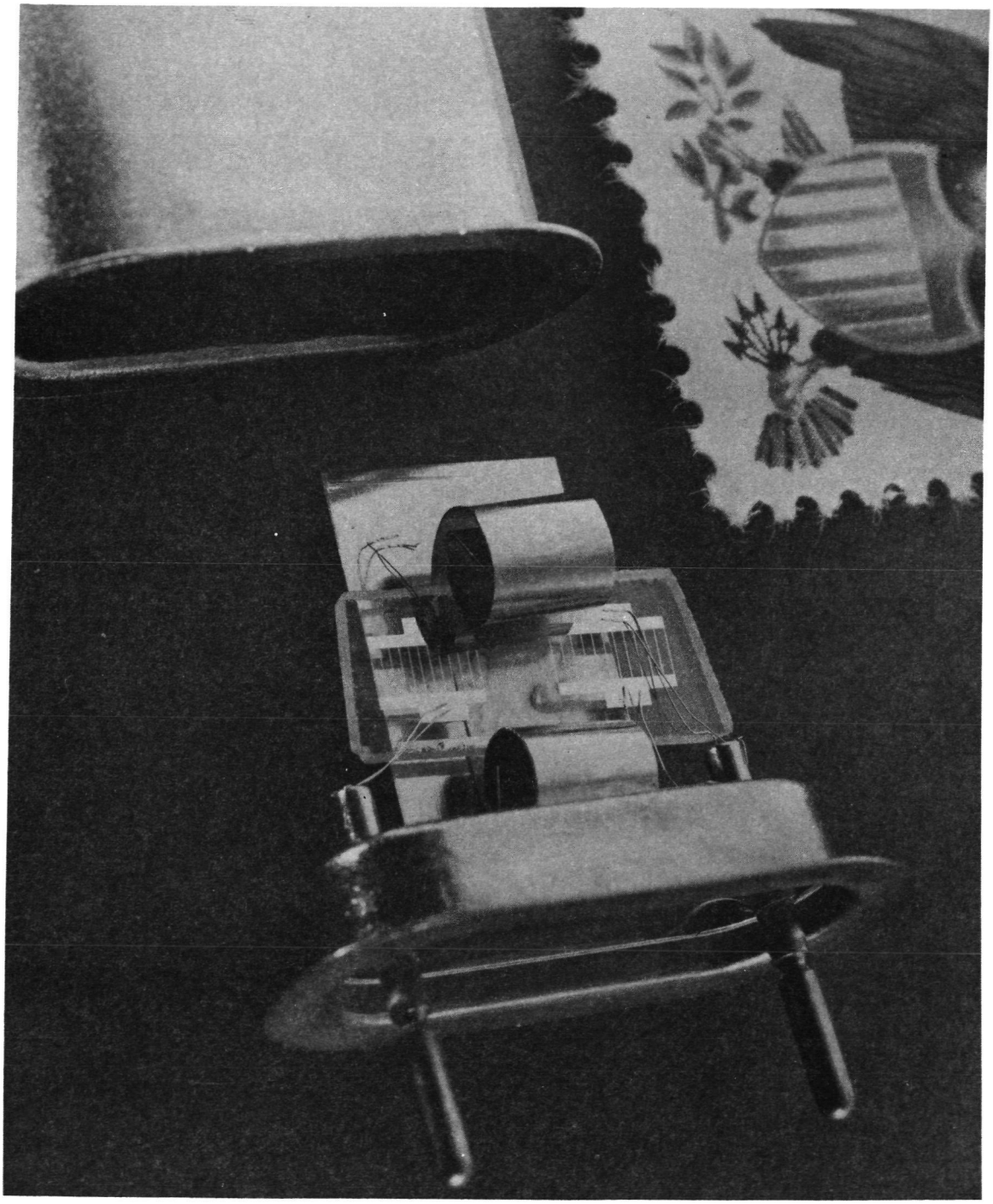

Figure 3.1 SAW Delay Line Mounted in HC36/U Package.

250°C for one-half hour in the ultraclean high vacuum sealing chamber. Upon return to Raytheon, the 10 sealed enclosures were checked for leaks and three were found to have leaks (all still functioned electrically). One of these three packages apparently did not seat correctly in the sealing dies because the base was deformed and the glass-to-metal seal was cracked. The other two packages with leaks showed no deformation or cracks, but both had similar scratch marks on the covers. The leaks were observed to be at the cover-to-base junction, so it is suspected that one of the five sets of dies had a burr on it. The three packages with leaks contained one aluminum, one gold, and unfortunately the only $SiO_2/LiTaO_3$ device. Thus we were left with five aluminum and two gold devices for testing.

3.2 Device Tests and Short-Term Frequency Stability

The first test performed on these devices was the determination of the distribution of frequencies. By the nature of the design of the delay lines, the oscillators can be tuned electrically over a range of about ±200 KHz. However, to obtain an estimate of the sensitivity to fabrication variables, the frequency of oscillation of each device was measured as each delay line was inserted in the same amplifier circuit board. The circuit board was set up to give oscillation near 401.2 MHz and was not changed as each delay line was inserted.

The five hermetic aluminum devices were tested and the RMS frequency deviation was found to be ±57 KHz. The largest deviation from the average frequency was 89 KHz and the smallest was 23 KHz. For three of the aluminum devices which were fabricated on the same substrate at the same time, the RMS deviation was ±35 KHz. The two gold devices were also checked, but a much larger spread on gold devices was found because the frequency is very sensitive to the gold thickness. For these devices the frequency changes by approximately 200 KHz per 100 Å of gold (more than 10 times larger than for aluminum devices). In general, a trimming step would be required during fabrication to adjust the gold thickness for the proper operating frequency. Since no attempt was made to trim these devices, the two sealed gold devices operated at 401.001 MHz and 400.802 MHz.

After the frequency distribution was measured, four of the sealed devices were baked at elevated temperatures (preaged). Three were baked at 100°C for 10 days and one was baked at 200°C for 7 days. Finally, the seven devices were mounted on individual circuit boards in preparation for the aging tests. The circuit layout for the aluminum devices is shown in Fig. 3 2. For the gold devices a UTO 513 amplifier was substituted for the UTO 503, since higher gain was required. At this point the temperature dependence of each completed oscillator was measured.

Before the aging tests were started, the short-term frequency stability (fractional frequency deviation) of each oscillator was measured for a 1-second count period. This was accomplished with a Hewlett-Packard 5360A Computing Counter and the results for the seven sealed devices are tabulated below.

Oscillator Number	Frequency Stability
2	1.0×10^{-9}
3	1.4×10^{-9}
4	6.6×10^{-10}
5	1.9×10^{-9}
6	1.3×10^{-9}
8	1.6×10^{-9}
9	1.2×10^{-9}

Recent research at Raytheon has shown that the short-term frequency stability can be improved by a factor of two to three by proper surface treatment of the SAW substrate. [3.1]

For the aging tests, the oscillators were placed in an environmental chamber which maintains a temperature of 20 ±1°C. Each day the frequency of each oscillator was measured to ±1 Hz and the temperature of each oscillator was measured by a thermocouple located near the SAW device. From the temperature versus frequency data recorded for each oscillator, corrections to the observed frequency were made for small temperature variations. Corrected frequency measurements were made five days a week, and then an average

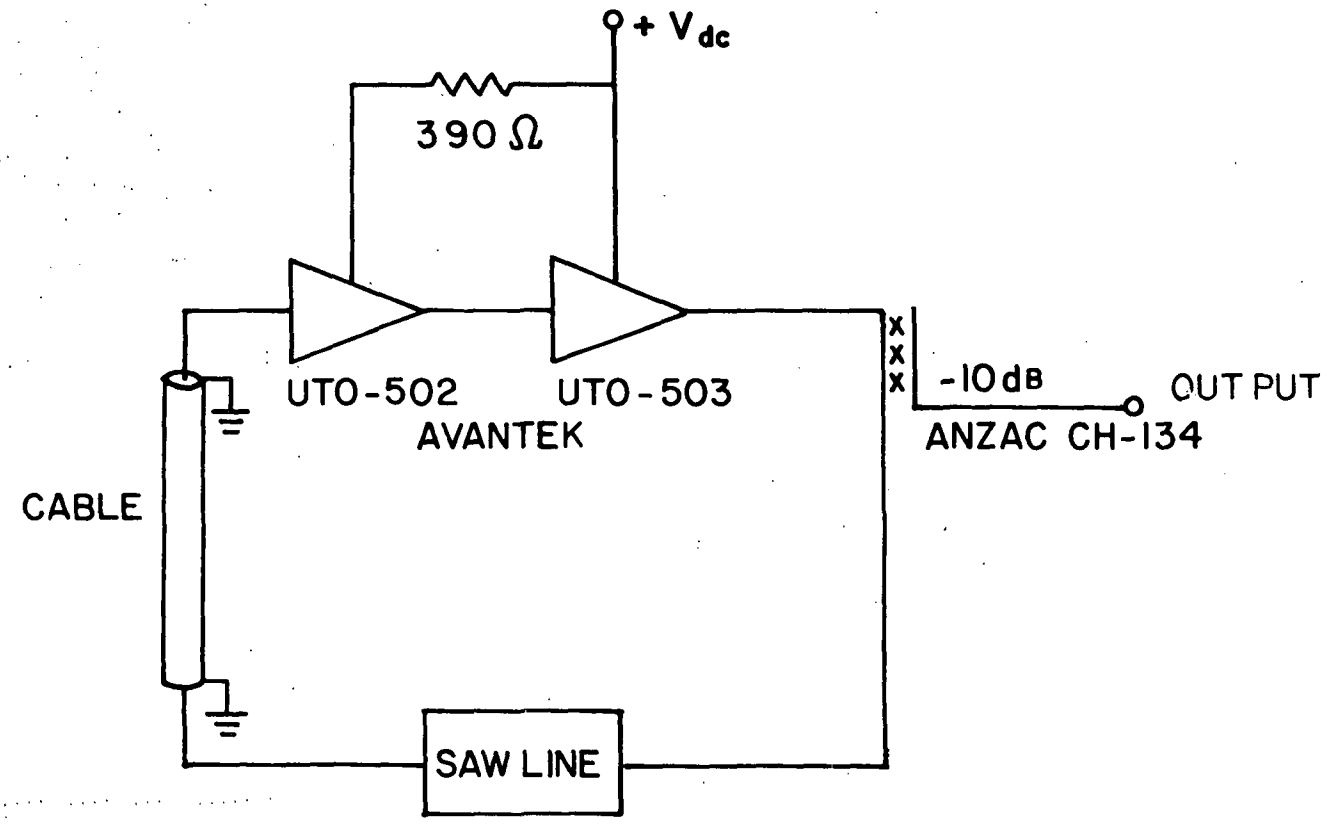

Figure 3.2 Circuit for a SAW Controlled Oscillator.

frequency for each week was calculated. Accurate calibration of the counter used to measure the frequencies was obtained from the 3.58 MHz color subcarrier boradcast on all network color TV programming. The color subcarrier frequency is 3.579534348 MHz and is maintained to an accuracy of p part in 10^{11}, as monitored by the National Bureau of Standards.

3.3 Aging Data

The weekly aging data measured for the seven devices sealed under this program is shown in Figs. 3.3 and 3.4. In addition, included in this data are two oscillators (No. 1 and No. 7) also sealed in HC36/U packages at ERADCOM, but at an earlier date, in cooperation with an internal Raytheon research program. Also, to enable a more complete analysis in the next section, aging data from the devices sealed in flatpacks during the first half of this program (and reported earlier)[3.2] is reproduced in Figs. 3.5 and 3.6. Included in Fig. 3.5 are three oscillators (No. 11, No. 16, and No. 17) sealed in flatpacks at an earlier date under Raytheon's internal research program. Table 3-1 gives a complete list of all 19 oscillators along with pertinent design and packaging information. This includes the type of transducer metal, package type, the atmosphere in the package, whether the device was preaged or not, and the time in weeks (T_{fs}) from transducer fabrication to the start of the aging test.

3.4 Analysis of Aging Data

An examination of the aging data in Figs. 3.3 to 3.6 quickly shows that aging is a complex process. Though most of the devices initially age upward, a number of the devices have changed direction of drift one or more times. This is a clear sign that more than one aging mechanism is present. The specific cause for the sudden turn to downward drift on three oscillators (No. 11, No. 12, and No. 13) has been identified as package leaks. All these devices tested as leaky at the end of the aging tests but did not leak at the start. The downward drift caused by a leaking package was clearly confirmed by oscillator No. 10, which is the HC36/U device with the cracked glass-to-metal seal. The aging of these four leaky devices is shown in Fig. 3.7.

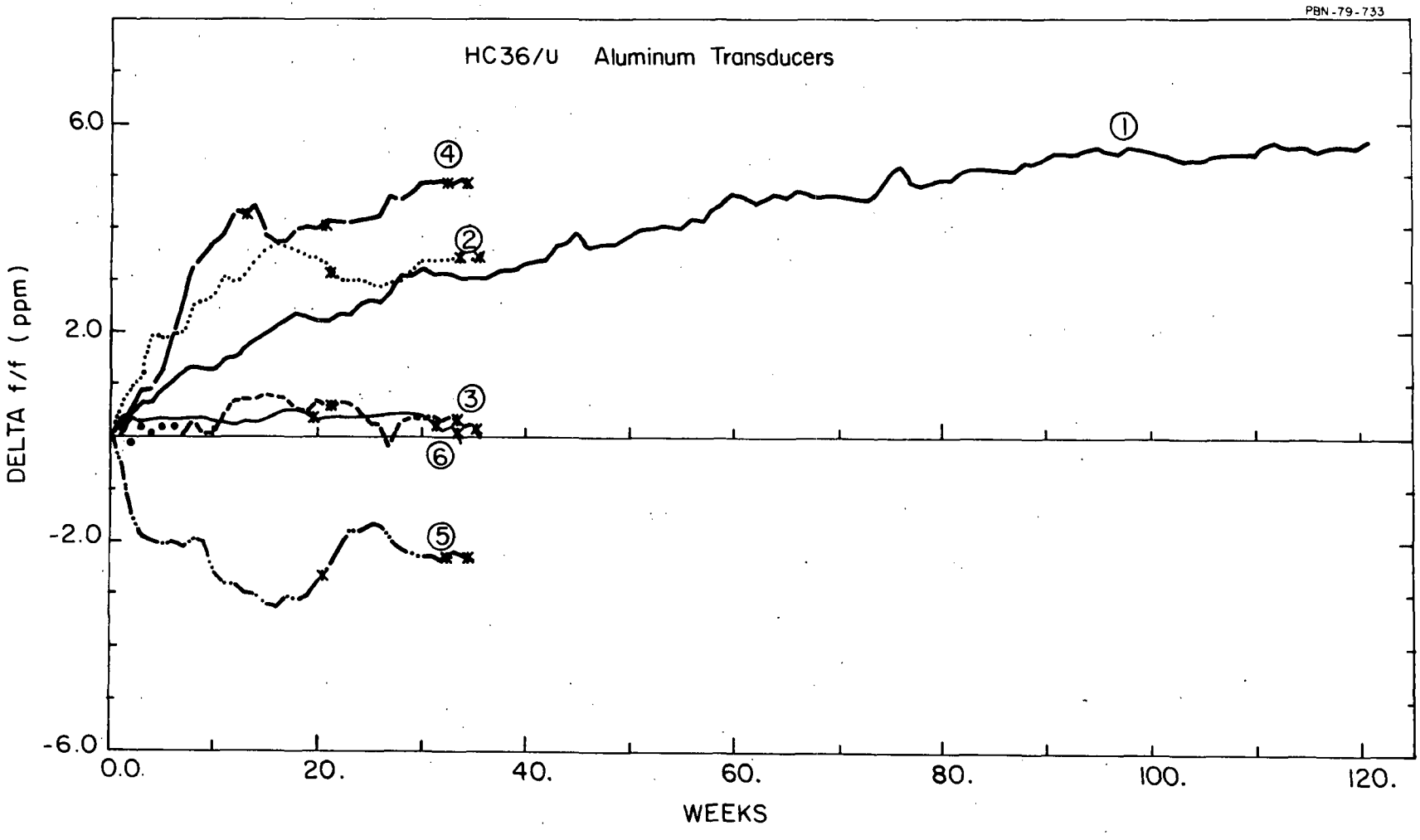

Figure 3.3 Aging Data for SAW Devices, with Aluminum Transducers, Sealed in HC36/U Enclosures. Asterisks (*) indicate the occurrence of a power interruption.

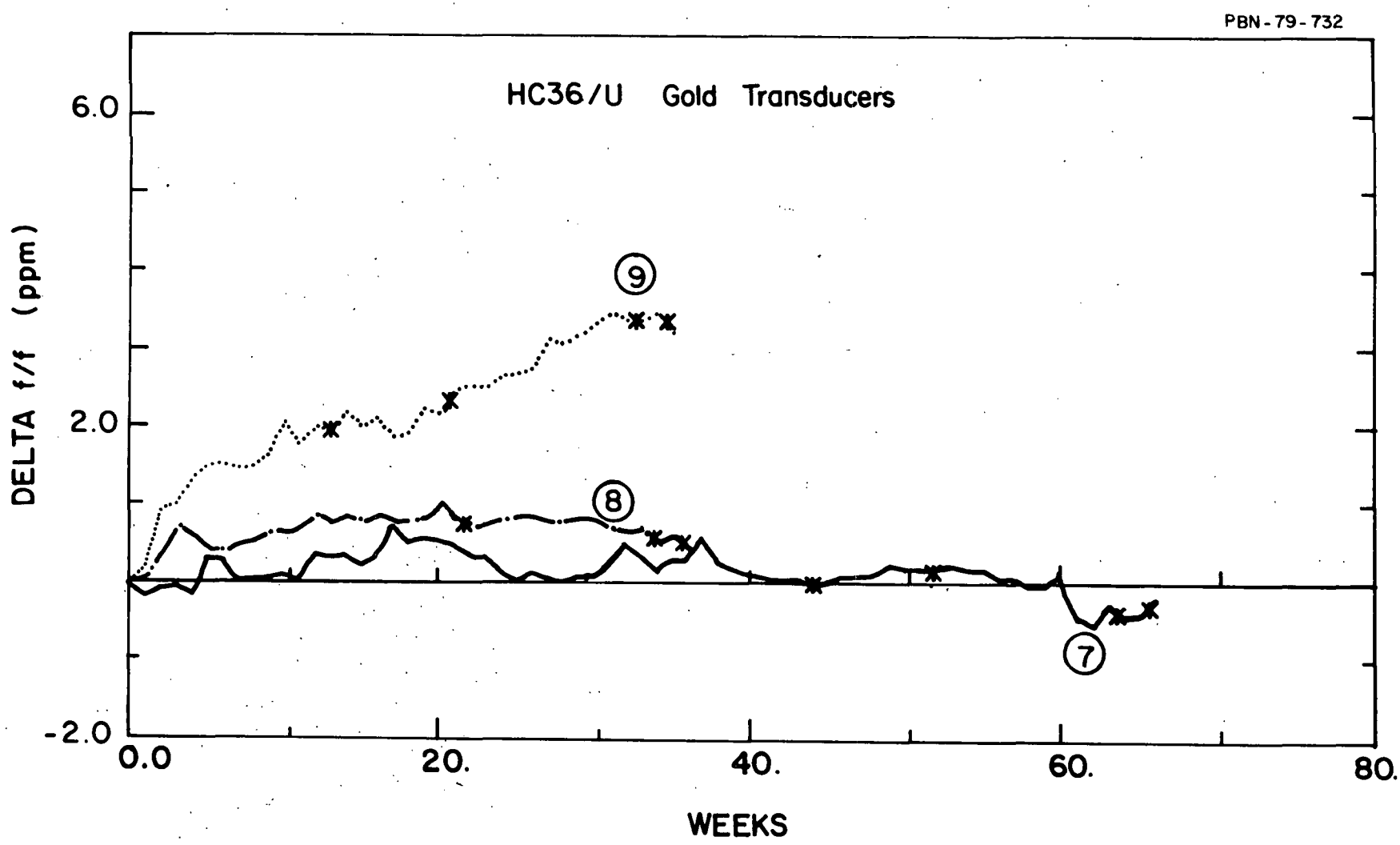

Figure 3.4 Aging Data for SAW Devices, with Gold Transducers, Sealed in HC36/U Enclosures.

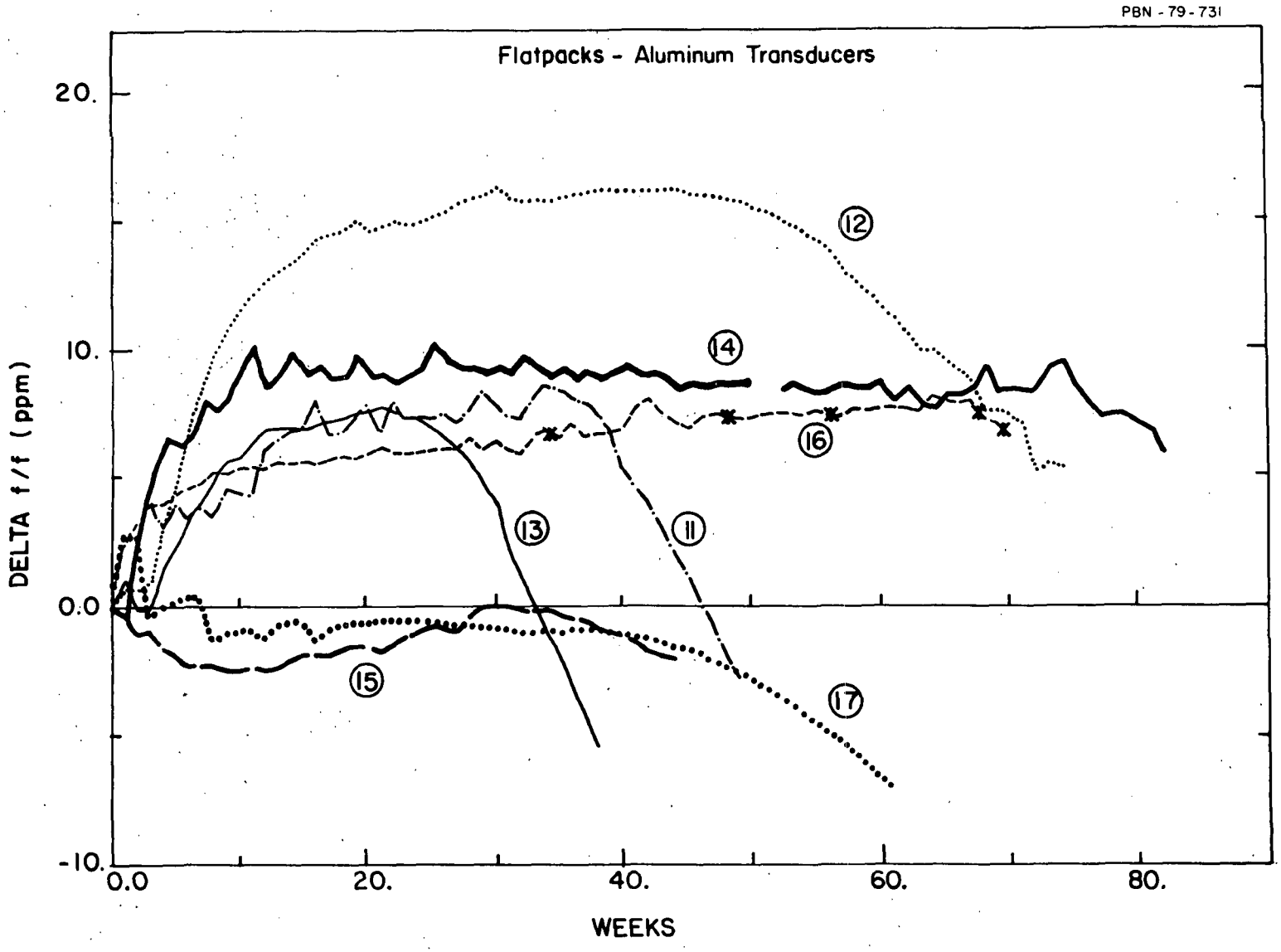

Figure 3.5 Aging Data for SAW Devices, with Aluminum Transducers, Sealed in Flatpacks.

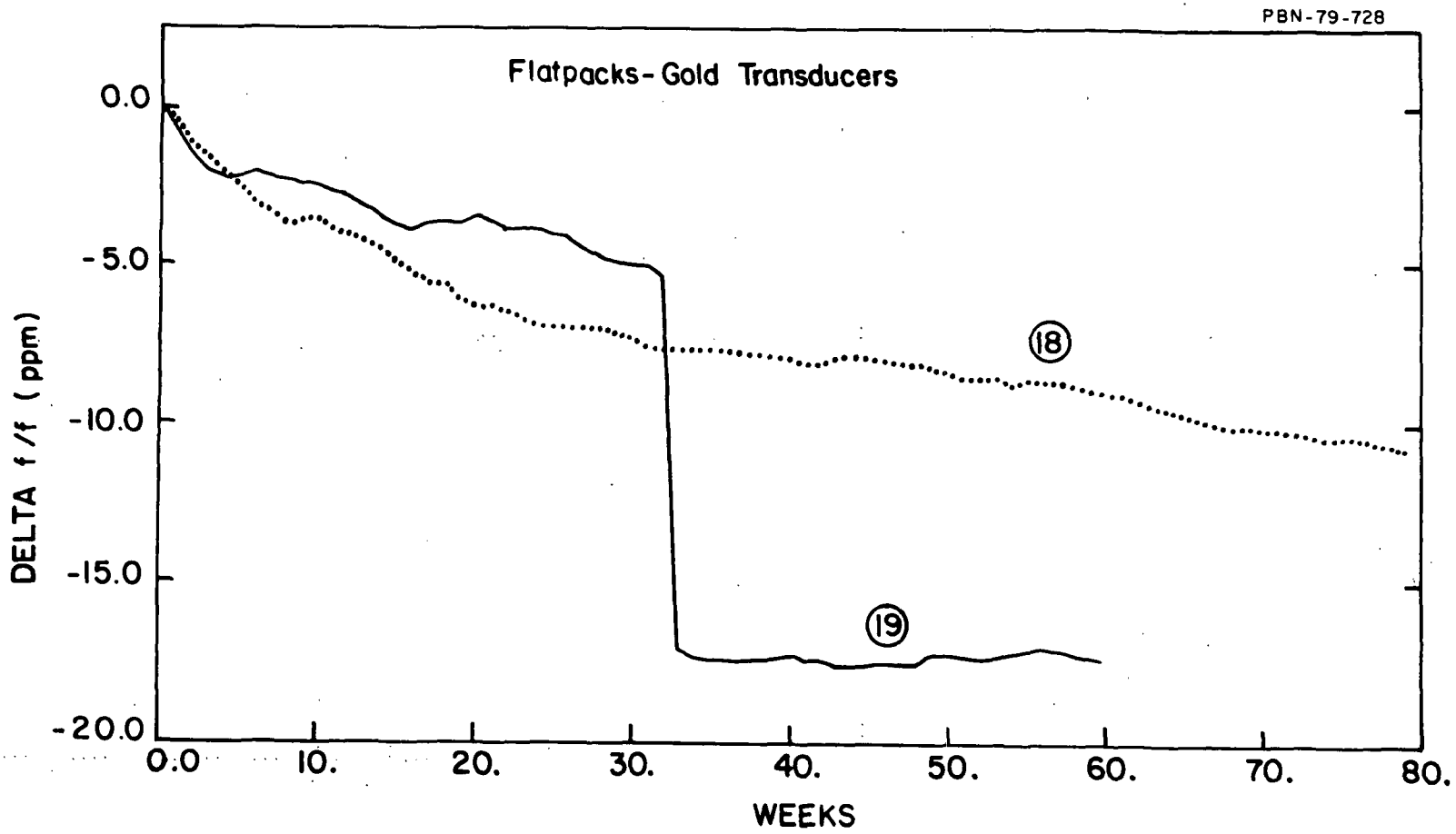

Figure 3.6 Aging Data for SAW Devices, with Gold Transducers, Sealed in Flatpacks.

TABLE 3-1

Osc. No.	Substrate Number	(MHz) Frequency	Transducer Metal	Package (Type Seal)	Atmosphere	Preaged	T_{fs} (weeks)
* 1	Q 514A	311	Cr-Al	HC36/U (Cold Weld)	Vacuum	No	~26
2	Q1089A	401	Al	HC36/U (Cold Weld)	Vacuum	No	6.3
3	Q1089B	401	Al	HC36/U (Cold Weld)	Vacuum	No	13.3
4	Q1089C	401	Al	HC36/U (Cold Weld)	Vacuum	Yes (10 days at 100°C)	7.3
5	Q1085C	401	Al	HC36/U (Cold Weld)	Vacuum	Yes (10 days at 100°C)	9.3
6	Q1093A	401	Al	HC36/U (Cold Weld)	Vacuum	Yes (07 days at 200°C)	6.3
* 7	QEC2	401	Au	HC36/U (Cold Weld)	Vacuum	No	~39
8	Q1088A	401	Au	HC36/U (Cold Weld)	Vacuum	No	6.3
9	Q1091B	401	Au	HC36/U (Cold Weld)	Vacuum	Yes (10 days at 100°C)	6.3
10	Q1088B	401	Au	HC36/U (Cold Weld)	Leak	No	....
** 11	Q514D	311	Cr-Al	Flatpack (brazed)	Vacuum	No	2.4
12	Q601A	401	Al	Flatpack (brazed)	Vacuum	No	0.9
13	Q617A	401	Al	Flatpack (brazed)	Vacuum	No	0.9
14	Q638A	401	Al	Flatpack (brazed)	Argon	No	1.9
15	Q638B	401	Al	Flatpack (brazed)	Vacuum	Yes (11 days at 90°C)	3.0
** 16	Q970A	401	Al	Flatpack (welded)	Nitrogen	Yes (11 days at 90°C)	3.9
** 17	Q969A	401	Al	Flatpack (welded)	Nitrogen	Yes (07 days at 90°C)	4.4
18	Q604	401	Au	Flatpack (brazed)	Vacuum	No	1.0
19	Q619B	401	Au	Flatpack (brazed)	Vacuum	No	2.7

* *Sealed at U. S. Army Electronics Command, Ft. Monmouth, New Jersey in cooperation with an internal Raytheon research program.*

** *Sealed under an internal Raytheon research program.*

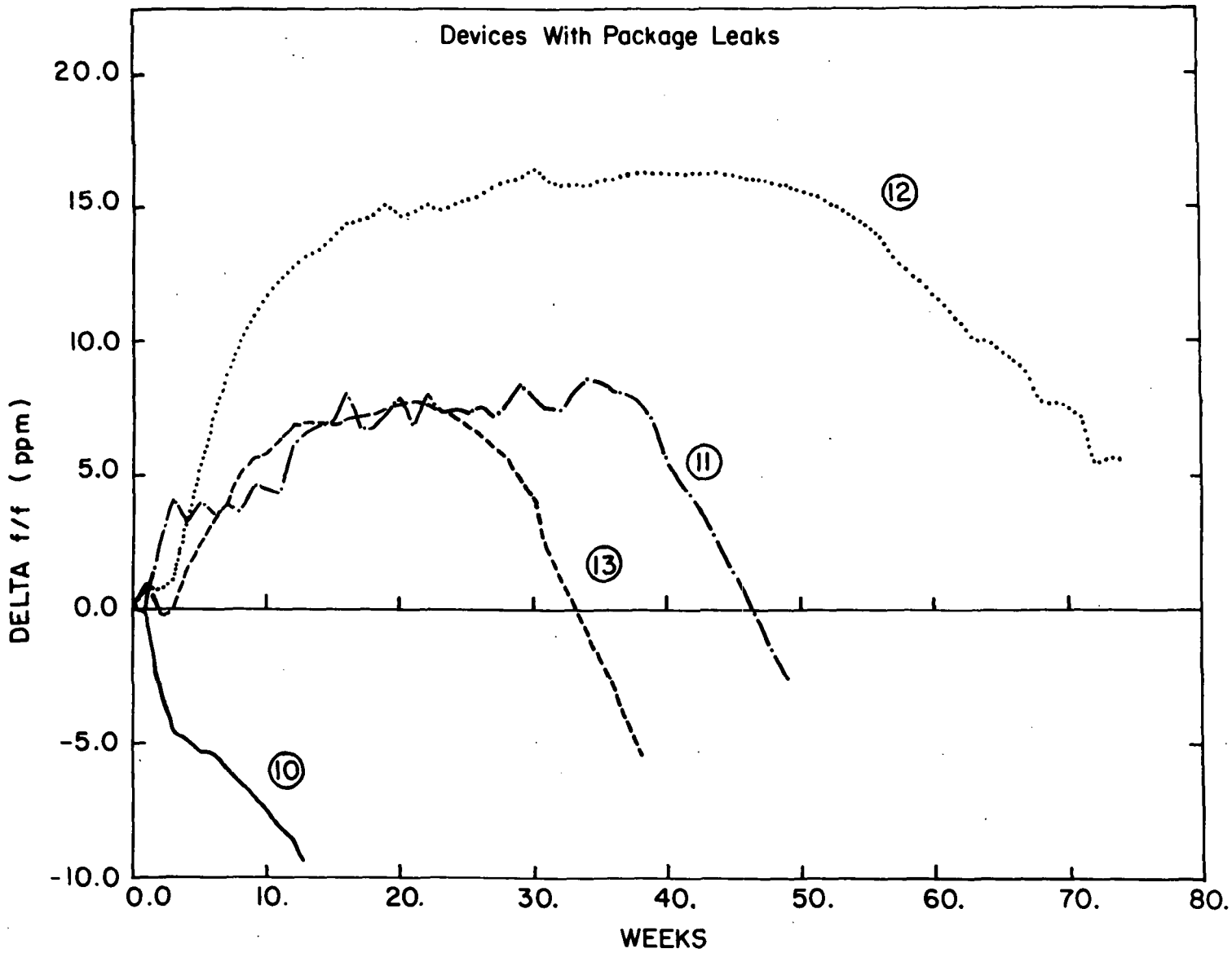

Figure 3.7 Aging Data for SAW Devices with Package Leaks.

Oscillator No. 10, which was known to have a leak at the start of the aging test, clearly shows a downward drift right from the beginning. Some of the four devices had leak rates near 10^{-4} cc/sec at 1 atmosphere, indicating that the packages filled up in a matter of days. The long, nearly linear, downward drift of the oscillator is most probably caused by the diffusion of moisture into the package followed by its adsorption on the quartz and metal surfaces. Oscillators 14 and 17 (not shown in Fig. 3.7) also showed a relatively steep downward drift but no leaks could be detected on these devices. This could mean either that the leaks were too small to be detected by the helium pressurization method or that there is some additional mechanism for downward drift. Note that only flatpacks have developed leaks and not a single HC36/U package has shown this problem.

Another important feature of the aging data in Figs. 3.3 to 3.6 is shown in Fig. 3.8. Here the total frequency drift after the first ten weeks of continuous operation for 14 of the 19 devices is plotted as a function of the time from transducer fabrication to the start of the aging test, T_{fs}. (Oscillator Nos. 5, 6, 10, 15, and 17 have not been included in Fig. 3.8 because they are special cases which are treated separately). The data in Fig. 3.8 clearly shows that the total frequency drift during the first ten weeks of aging is smaller for the devices with large values of T_{fs} (see Table 3-1 for values of T_{fs}). Since the time from sealing to start of the aging tests was approximately the same for all of the devices (slightly longer for the three preaged devices) and in only one case (Oscillator No. 3) exceeded four weeks, the evidence strongly indicates that the relaxation process which causes this initial aging starts at the time of transducer fabrication and not at the time of sealing. Even though the larger values of T_{fs} occurred only for devices in the HC36/U package, the decreasing trend is clearly present within a single package type. In fact, the data suggests that the initial aging in the first ten weeks is probably independent of package type. If this is the case, the dominant aging process must be inherent in the SAW device, and not a packaging-related problem. This is true, however, only as long as gross contamination problems such as package leaks or outgassing from mounting material are not present.

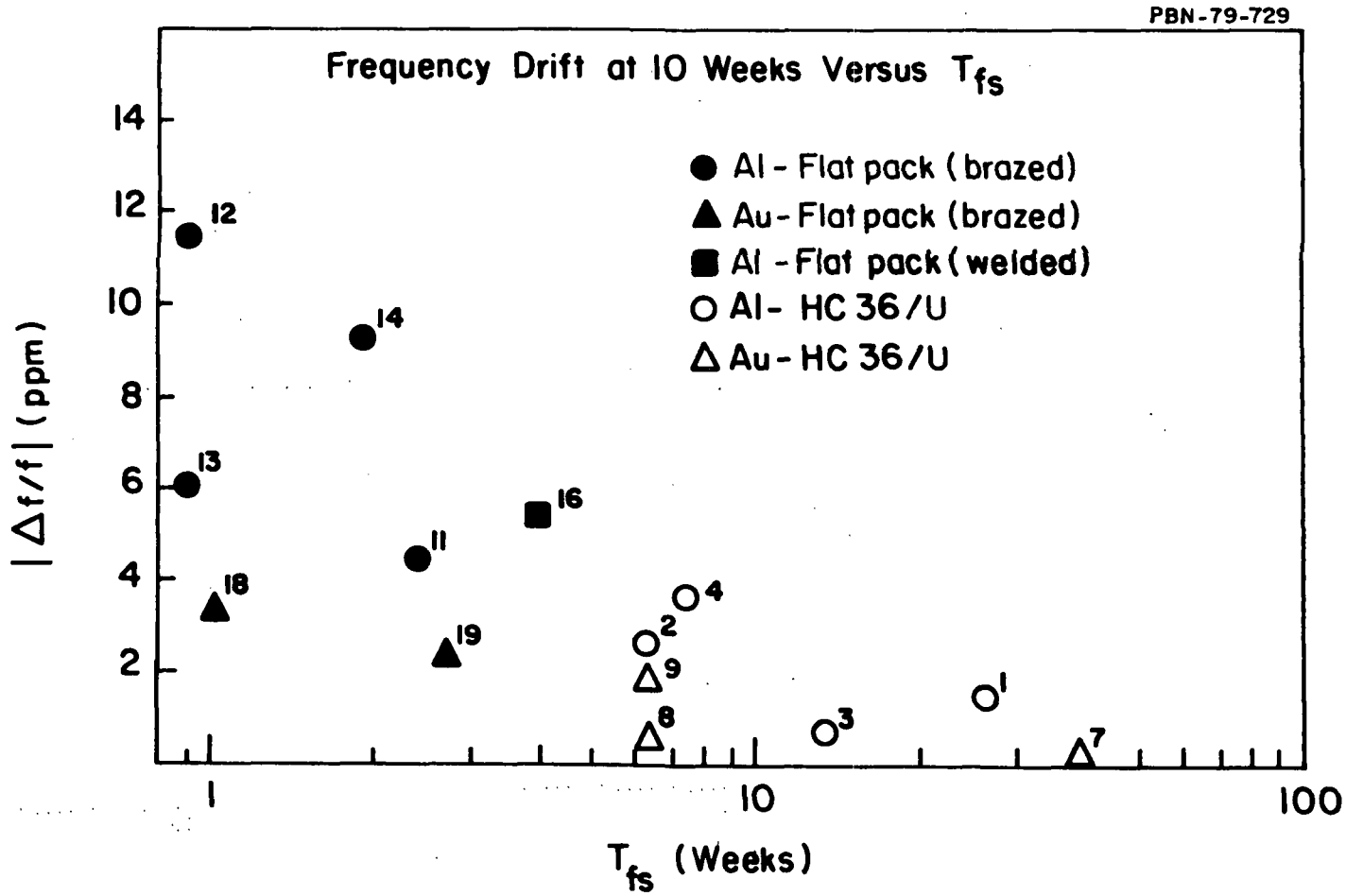

Figure 3.8 Frequency Drift in First Ten Weeks As a Function of the Time from Transducer Fabrication to Start of the Aging Test, T_{fs}. The numbers refer to the oscillator from which the data point was derived.

Though the initial aging may not be strongly package dependent, a closer look at the frequency drift of the aluminum devices (Figs. 3.3 and 3.5) shows that aging is sensitive to the temperature environment after sealing. This is illustrated by five oscillators (Nos. 4, 5, 15, 16, and 17) that were baked at 90 to 100°C for 7 to 11 days, after sealing (See Table 3.1). Oscillators 4 and 16 aged upward in a manner similar to nonpreaged devices, but oscillators 5, 15, and 17 all displayed a consistent tendency to age downward initially, followed by a slight increase or leveling off, and then finally a downward trend again. This complex downward aging is seen for both package types, but it only occurs for preaged aluminum devices. However, as pointed out above, not all preaged devices show this complex behavior. Among the unpreaged devices, the trend is to age upward but at a decreasing rate. Though there is some irregularity in the data, the upward drift is clear for both package types. The magnitude of the drift is less in the HC36/U devices; however, as just discussed, this may be primarily due to the longer time between fabrication and start of testing.

Two of the aluminum devices in HC36/U packages (Nos. 3 and 6) deserve special comment. Oscillator No. 3 was operated only 24 hours per week for the first seven weeks of the aging test. The frequency was recorded at the end of each 24 hour "on" period and then the oscillator was turned off for six days, whereupon the cycle was repeated. The data accumulated during the period of intermittent operation is shown by large dots in Fig. 3.3. The aging, after continuous operation was started, was clearly less than for similarly packaged devices. It is puzzling why no drift was seen during the intermittent operation, but otherwise the data confirms that "on the shelf" storage for a number of weeks will yield lower aging. The other oscillator of particular interest is No. 6. This oscillator is unique in that it was preaged at 200°C for seven days and has shown the lowest aging of any aluminum device. Experience with preaging at 100°C strongly suggests the need for more data, but nevertheless the result is very encouraging.

The five devices with gold transducers behaved very differently from the aluminum devices, in that they showed distinctly different aging characteristics for the two packaging techniques (Figs. 3.4 and 3.6). In the flatpack, the aging was downward and relatively large in magnitude. In the HC36/U packages, the aging was smaller and generally upward. Oscillator No. 7 has the largest value of T_{fs} ($\sim$ 39 weeks) and has the lowest aging of all the gold devices. Also of interest is the fact that oscillator No. 9, which was preaged at 100°C for ten days, shows the largest aging of the three gold devices in HC36/U packages.

Interpreting the aging data of the gold devices is difficult because of the different characteristics between package types. However, the fact that devices with gold transducers age differently from aluminum devices reinforces the hypothesis that the transducers are the source of the aging process in aluminum devices. The data for gold devices in Fig. 3.8 suggests that long periods between fabrication and the start of operation give lower aging. However, the fact that there was a sign change from flatpacks to HC36/U package makes this conclusion somewhat less certain.

During the course of the aging test a number of power outages occurred, causing an interruption in the operation of the oscillator. In the current devices these interruptions are indicated by asterisks on the aging data. In most cases the interruptions were short ($\sim$10 minutes); however, the two most recent ones (e.g. $\sim$ weeks 30 to 35 in Fig. 3.3) lasted for several days each. In addition, a 2½ week interruption occurred for oscillator No. 14 (gap at weeks 50 to 53 in Fig. 3.5) when it was intentionally turned off to observe the affect of a long interruption. In many cases the interruptions resulted in small perturbations of much less than 1 ppm, but there has been no sign of a major disruption of the aging process. In no case has there been any evidence of a retracing of previous frequency drift.

3.5 Mathematical Modeling of the Aging Data

In the course of numerous aging studies on quartz crystal resonators,

three mathematical models have been identified with specific aging processes. The most commonly observed model is logarithmic,[3.3] in the form of equation 3-1.

$$\frac{\Delta f}{f} = A \text{ Log } (B t + 1) \qquad (3\text{-}1)$$

Here $\Delta f/f$ is the fractional frequency change, t is time, and A and B are constants relating to the aging process. Physical processes that follow a logarithmic rate are chemisorption, oxidation, and internal stress relaxation.

Another commonly observed model has an exponential form,[3.3] as shown in equation 3-2.

$$\frac{\Delta f}{f} = A(1-e^{-Bt}) \qquad (3\text{-}2)$$

This corresponds to first order chemical reactions and to adsorption or desorption of a physisorbed monolayer. This last process tends to occur over relatively short periods (days) and may be reversible.

Finally, a third model has been identified with diffusion through thin films[3.4] and has the form of equation (3-3).

$$\frac{\Delta f}{f} = A(t)^B \qquad (3\text{-}3)$$

In diffusion processes the value of B is typically close to 0.5.

A computer program for doing a least mean squares fit to these three functions was used to evaluate the three models for our aging data. Since the program would fit only one model at a time, the devices which showed a systematic change in aging direction could not be used since the change in sign means more than one process is present. Some of the devices also showed so little drift that random scatter dominated the aging curve. No attempt was made to fit these curves either. In all, five oscillators were analyzed to find the model that fit best.

The result of this analysis showed that the logarithmic model provided the best all-around fit. In some individual cases it did not give the best fit, but it was always either first or a very close second. In addition, the other two models gave a very bad fit in at least one or two cases. Furthermore, the observation that the logarithmic model fits best is consistent with published results on SAW resonators.[3.5] Figs. 3.9 to 3.13 show the aging data and the fitted log curves for five oscillators. In each figure the RMS deviation (in ppm) and the values for A and B are shown for the fitted curve.

The physical interpretation of the constants A and B in equation 3-1 is that A is related to the activation energy of the process and B is related to the initial condition at the start of the process. The dependence of B on initial conditions can be demonstrated by considering the form equation 3-1 takes if the observation of the relaxation process does not start at t = 0 but at some later time t_o. In that case the observed fractional frequency change $\frac{\Delta f'}{f}$ is given by equation 3-4.

$$\frac{\Delta f'}{f} = \frac{\Delta f}{f} - \frac{\Delta f_o}{f} = A \text{ Log } (Bt + 1) - A \text{ Log } (Bt_o + 1) \qquad (3\text{-}4)$$

The time relative to the start of the observation is t', and is given by

$$t' = t - t_o \qquad (3\text{-}5)$$

where t is the time from the start of the relaxation process. Using equation 3-5 to express $\frac{\Delta f'}{f}$ in terms of t', equation 3-4 reduces to

$$\frac{\Delta f'}{f} = A \text{ Log } (B't' + 1) \qquad (3\text{-}6)$$

where

$$B' = \frac{B}{Bt_o + 1} \qquad (3\text{-}7)$$

Note that equation 3-6 has exactly the same form as 3-1 except that t becomes t' and B becomes B'. Also note that for $t_o > 0$, B' decreases from an initial value of B to an eventual value of $\frac{1}{t_o}$. Thus we find that the value

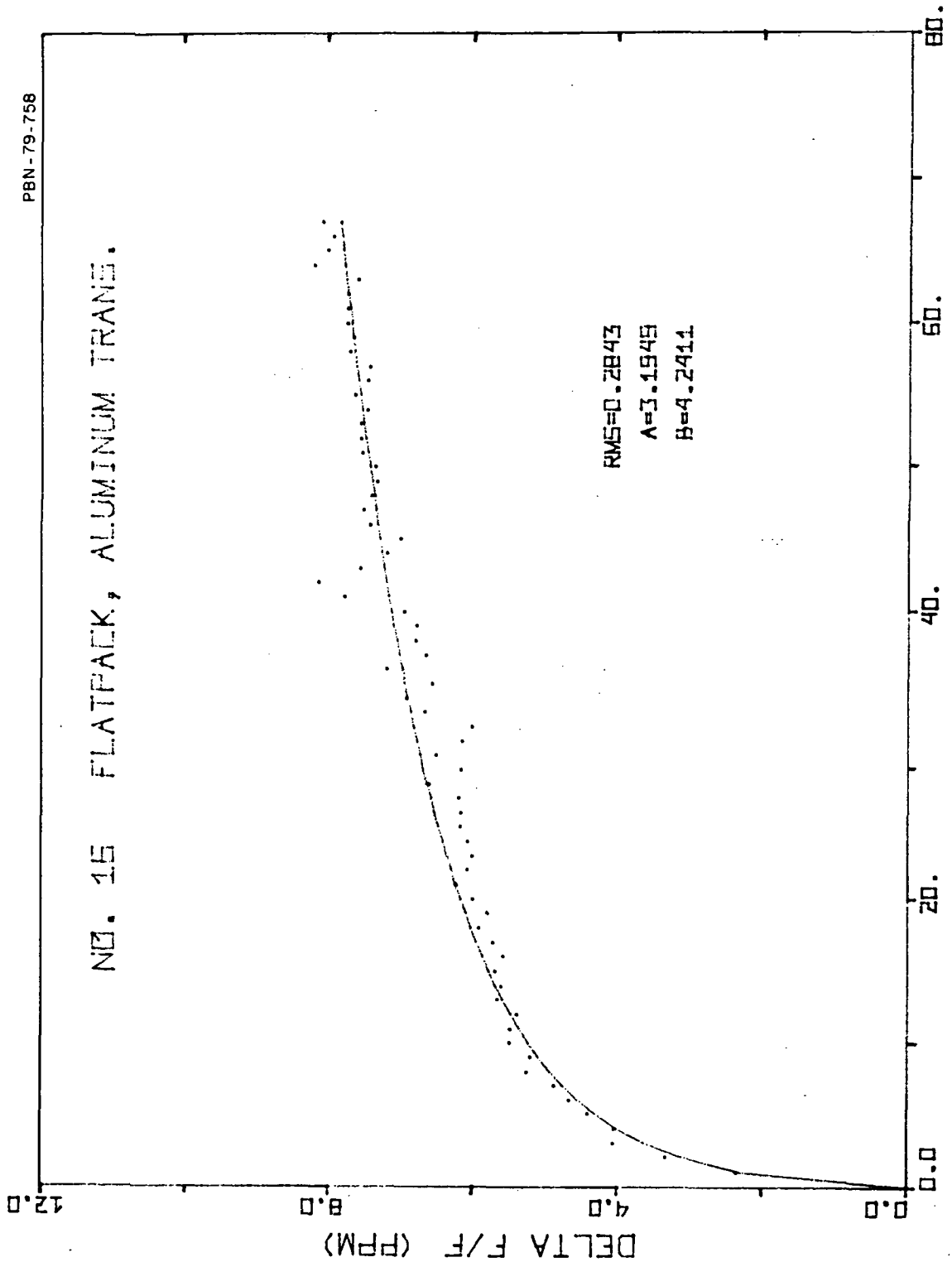

Figure 3.9 Log Fit to Aging Data.

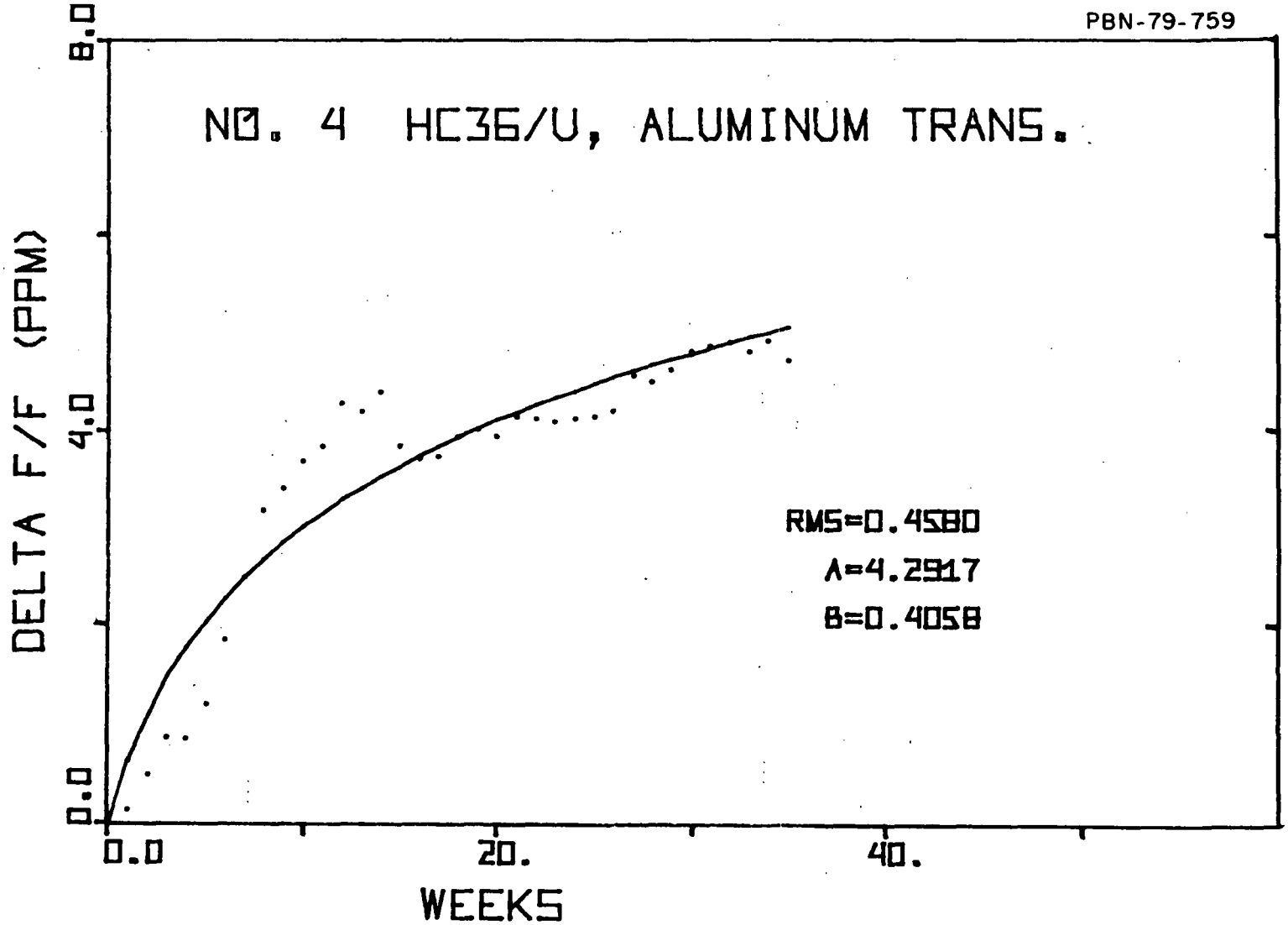

Figure 3.10 Log Fit to Aging Data.

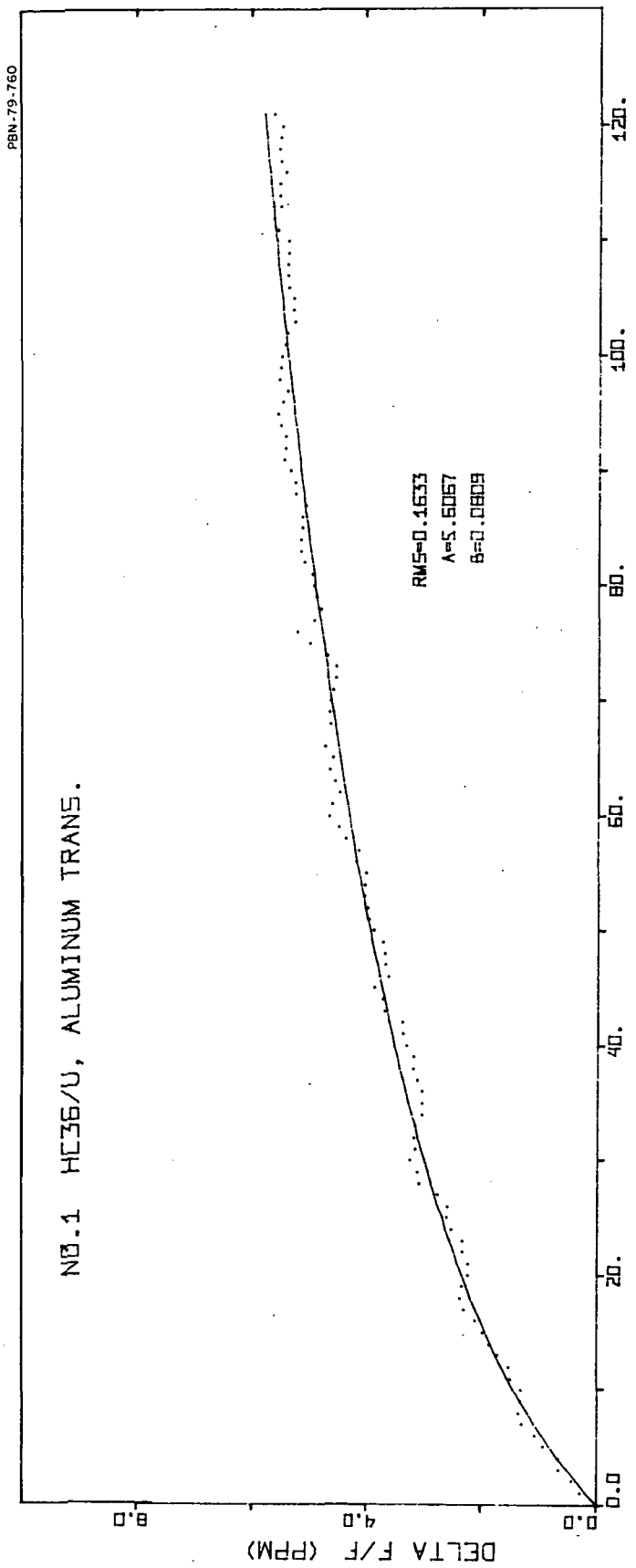

Figure 3.11 Log Fit to Aging Data.

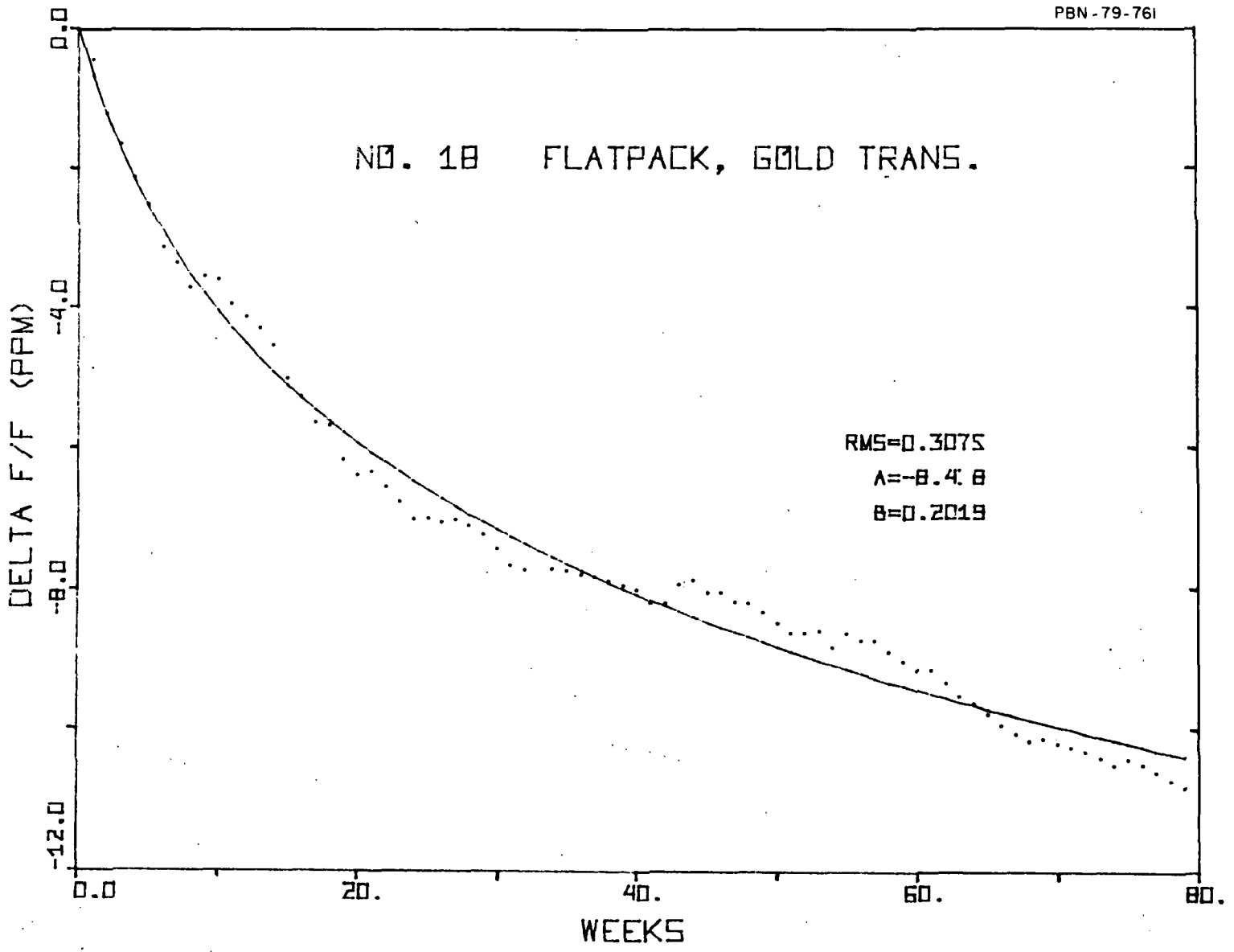

Figure 3.12 Log Fit to Aging Data.

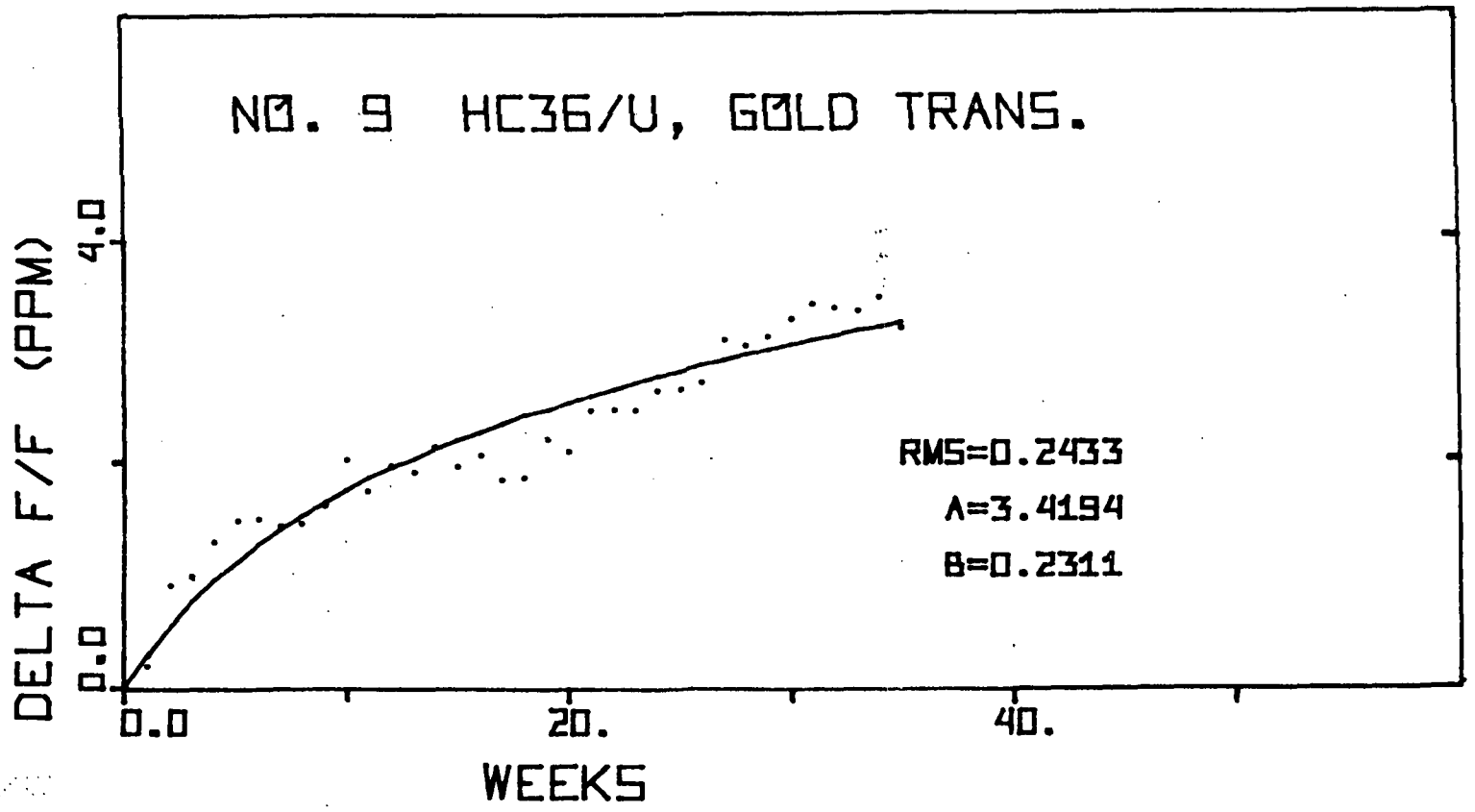

Figure 3.13 Log Fit to Aging Data.

of A does not depend on the value of t_o, but that the value of B' decreases as the time from the start of the relaxation process to the observation increases.

With the above result in mind, it is interesting to note how the calculated values of B decrease from Fig. 3.9 to Fig. 3.11. These devices are all aluminum and it is evident that large values of T_{fs} result in small values of B. (The variable B in the figures actually corresponds to B' in equation 3-6.) It is not clear that T_{fs} is equivalent to t_o, since the relaxation process may not proceed at the same rate when the device is oscillating as compared to a nonoperating state. In fact the evidence is that T_{fs} and t_o are not equivalent, since B for oscillator No. 1 is not equal to $1/T_{fs}$. Though the calculated values of B change by nearly two orders of magnitude, the values of A vary by little more than a factor of 2 among all five devices. This is consistent with our conclusion above that A does not change with the time of observation.

Our analysis of curve fitting has provided strong evidence that the aging process on SAW delay lines follows a logarithmic function of time and it has also provided further evidence that the aging process starts at or near the time of transducer fabrication. There are several possible mechanisms that produce a logarithmic function, and it is uncertain at this time which one it is.

Previously published data[3.6] indicates that oxidation of aluminum is not a large enough effect to cause the observed frequency shifts, and of course oxidation does not occur with gold transducers. Chemisorption is also not likely, since similar aging rates were observed for packages with different atmospheres and wide degrees of cleanliness. (The flatpacks for oscillator No. 16 and No. 17 were simply sealed in a plastic dry box flushed with dry nitrogen.) The most likely mechanism is the relaxation of internal stress in the transducer metallization. This would, of course, start at or near the time of transducer fabrication and is very likely to be sensitive to heat treatment, as has been observed.

3.6 Conclusions

The devices packaged in HC36/U cold weld enclosures have shown lower aging than similar devices sealed in flatpacks. Part of the reason for this lower aging is the development of leaks in the flatpacks which resulted in a rapid decrease in frequency. The HC36/U enclosures showed no problem with leaks and the evidence is strong that the cold weld technique is of high enough quality that the dominant aging mechanism is now inherent in the SAW device and is not package related. The aging data accumulated under this program clearly shows that the frequency drift decreases with increasing time from transducer fabrication to start of the aging test. This characteristic is also probably partly responsible for the lower aging of the cold weld devices, since the time period from fabrication to sealing was somewhat longer than for the flatpacks.

The observations that (1) the initial aging decreases with increasing values of T_{fs}, (2) gold devices age differently from the aluminum devices, and (3) decreasing values of B reflect long periods of relaxation before observation, all support the hypothesis that the dominant aging mechanism on the delay lines with aluminum transducers is confined to the SAW device itself and starts at or near the time of transducer fabrication. A likely candidate for this mechanism is the relaxation of internal stress in the transducer metal, but this has not been confirmed yet.

The effect of preaging at elevated temperatures after sealing has resulted in a rather complex aging curve for some (but not all) of the devices preaged at 100°C. The one device preaged at 200°C has shown the lowest amount of frequency drift of all the devices, a very encouraging result. Furthermore, it is clear from the aging data that storing unsealed devices at room temperature for 15 to 20 weeks can yield low aging devices.

REFERENCES

3.1 T. E. Parker, 1/f Phase Noise in Quartz SAW Devices," Electronics Letters, 15, 296, 1979.

3.2 T. E. Parker, "Surface Acoustic Wave Stabilized Oscillators," Final Report NAS5-23701, September 1976 to December 1976, Raytheon Research Division, Waltham, Massachusetts, Jan. 1978.

3.3 A. W. Warner, D. B. Fraser, and C. D. Stockbridge, "Fundamental Studies of Aging in Quartz Resonators," IEEE Trans. on Sonics and Ultrasonics, SU-12, 52, 1965.

3.4 G. L. Dybwad, "Aging Analysis of Quartz Crystal Units with TiPdAu Electrodes," Proc. 31st Symp. on Frequency Control, 144, 1977.

3.5 W. R. Shreve, J. A. Kusters, and C. A. Adams, "Fabrication of SAW Resonators for Improved Long Term Aging," 1978 IEEE Ultrasonics Symp., 573, 1978.

3.6 T. E. Parker, "Aging Characteristics of SAW Controlled Oscillators," 1977 IEEE Ultrasonics Symposium, 862, 1977.

4.0 TASK II - TEMPERATURE COMPENSATION

4.1 Oscillator Configuration

The general layout for the SAW delay line oscillator and temperature compensation circuitry is shown in Fig. 4.1. The basic oscillator consists of a SAW delay line in series with a high-gain amplifier and voltage-controlled phase shifter. The condition for oscillation is that the net phase shift around the loop must be an integral multiple of 2π or

$$\phi_{SAW}(T) + \phi_{P-S}(T) + \phi_{AMP}(T) = 2n\pi, \; n = 1, 2, \ldots \qquad (4\text{-}1)$$

where ϕ_{SAW}, ϕ_{P-S}, and ϕ_{AMP} are the temperature dependent phase shifts through the delay line, phase-shifter, and amplifiers respectively. Because $\phi_{SAW}(T) = -\omega\tau(T)$ where τ is the delay time of the SAW device, the above equation determines the oscillation frequency at any given temperature. The oscillator frequency will remain constant, provided that the phase shifter exactly mirrors the phase changes introduced by the delay line and amplifier as the temperature changes.

4.2 Delay Line Temperature Characteristics

The most widely used family of quartz orientations for SAW delay lines is the rotated Y-cut. All of these cuts have in common extremely parabolic phase versus temperature characteristics over a wide range of temperatures, with the turnover temperature or minimum phase temperature dependent on the specific cut.[4.1] In our experiments we used a +40° rotated Y-cut which has a turnover temperature around 40°C. As we shall show, when this Y-cut is used in conjunction with the remainder of the oscillator circuit, an effective turnover temperature of about 20°C is obtained.

Because of the highly parabolic nature of the temperature dependent phase shift associated with the delay line, and also because of the commercial availability of an extremely linear voltage controlled phase shifter (Merrimac #PSEF-3E-400), the problem of compensation reduced primarily to one of generating a quadratic voltage versus temperature bias signal to drive the phase shifter. These relationships are shown schematically in Fig. 4.1. Further, in

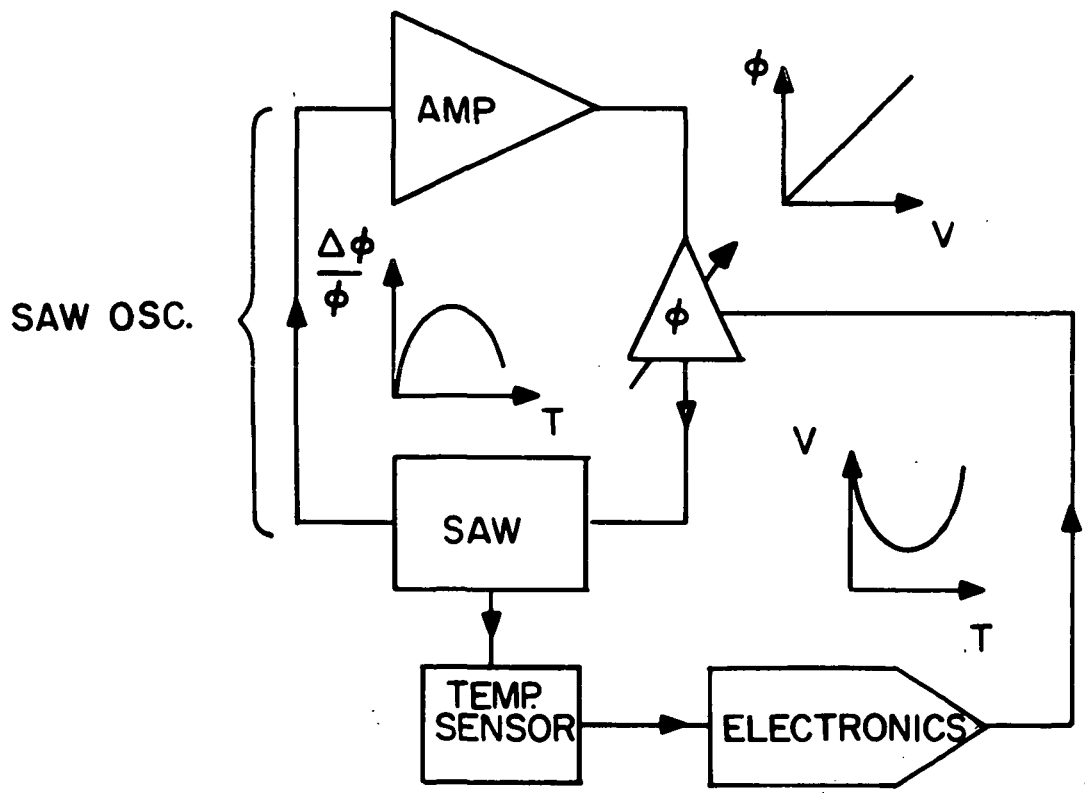

Figure 4.1 SAW Delay Line Oscillator with Electronic Temperature Compensation.

order to limit power requirements for the oscillator as a whole, an effort was made to minimize the power consumption of the temperature compensation circuitry. Two general classes of compensation methods were explored, active and passive analog-type circuits.

4.3 Passive Compensation Techniques

Passive compensation circuits provide a low power and inexpensive means of introducing an order of magnitude improvement in the frequency vs temperature characteristics of SAW oscillators. These circuits typically consist of one or more resistors and thermistors arranged in some type of a voltage divider circuit.[4.2-6] By properly choosing resistance values, we may obtain quasiparabolic voltage versus temperature characteristics. Figure 4.2 shows the simplest circuit tested, consisting of two identical thermistors, two resistors, and two battery supply voltages.[4.6] The solid curve indicates the control voltage that was necessary to apply to the phase shifter in order to maintain constant oscillator frequency. Increasing and decreasing temperature, $\sim$1.5°C/min. are indicated by arrows on the solid curves. The hysteresis indicated will be discussed in Sec. 4.5. The dashed line indicates the response obtained from the passive circuit. Component values for the compensation network were chosen to give a least squares fit with respect to the solid curves. For sufficiently small temperature fluctuations about the minima, as shown in Fig. 4.2, the generated curve is quite parabolic. However over the larger temperature excursions required for this program, significant deviations from parabolicity exist.

The appropriate control voltage was determined using the phase-lock loop circuit shown in Fig. 4.3. A stable rf signal at the desired oscillator operating frequency obtained from a reference oscillator is mixed with the output from the SAW oscillator. The phase difference between the two signals is detected and is amplified by a low-pass, high-gain amplifier. The amplified signal drives the voltage controlled phase shifter within the SAW oscillator and biases it at the point for which both reference and SAW oscillator frequencies are equal. This control voltage is then measured as a function of SAW delay line temperature.

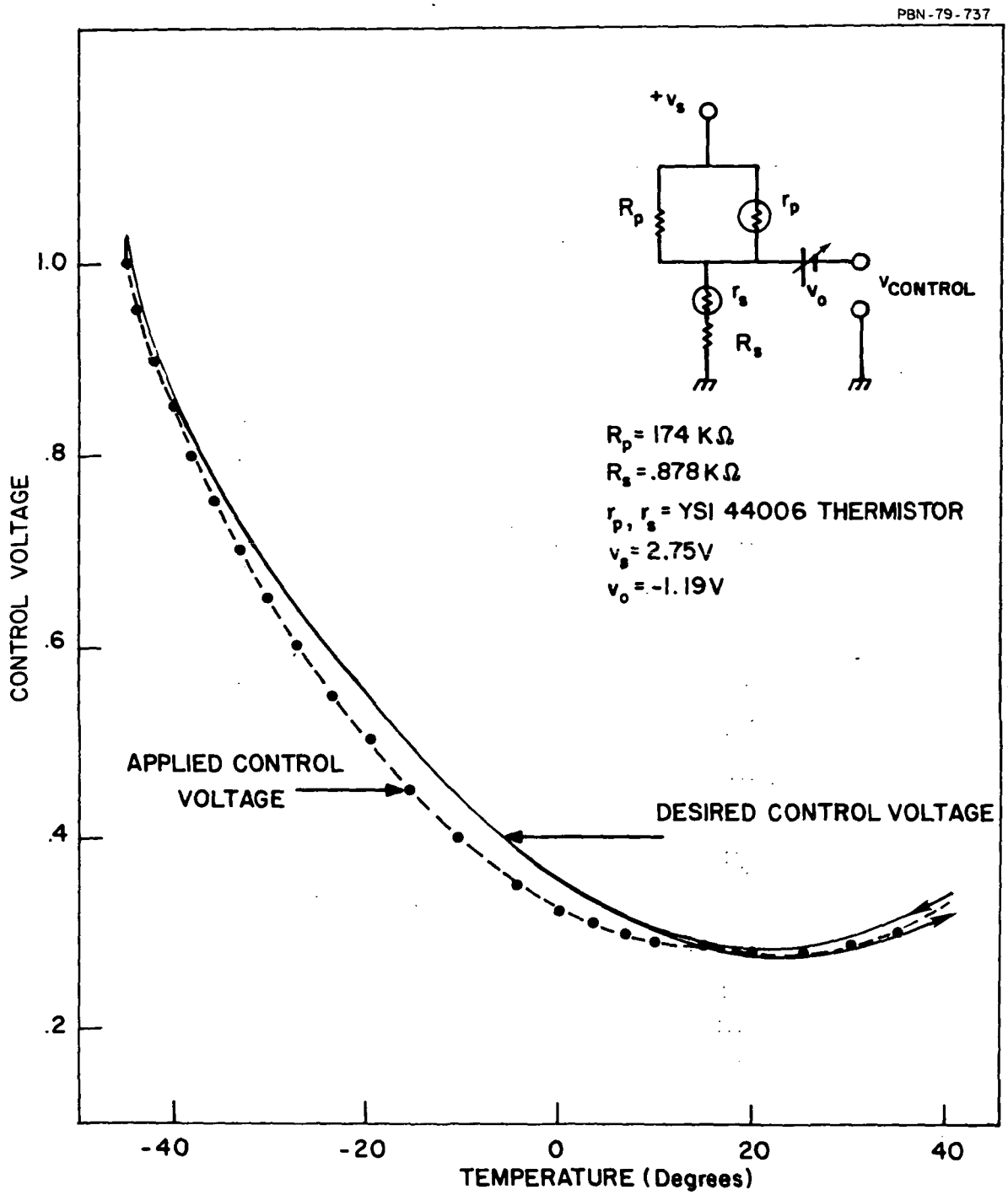

Figure 4.2 Passive Compensation Circuit. Solid curve represents control voltage needed for constant frequency. Dot-dashed curve represents actual generated voltage.

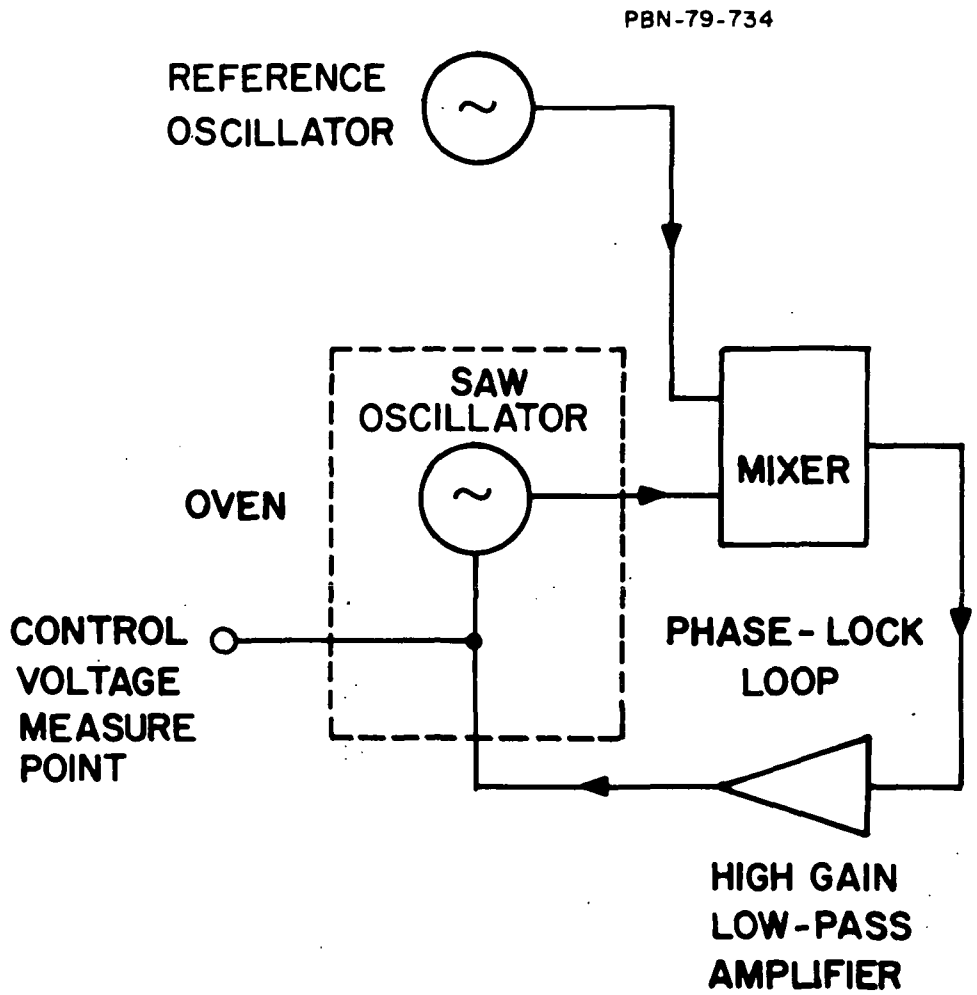

Figure 4.3 Phase-Lock Circuitry Used to Determine Control Voltage for Fixed Frequency.

As shown in Fig. 4.4, frequency compensation to within about 15 ppm was obtainable using this technique while drawing about 0.7 mW of power from a 2.75 V supply. In an attempt to obtain a more nearly quadratic curve over the entire temperature range, different passive networks using as many as three thermistors and three resistors were analyzed numerically, but it was found that no significant improvement in parabolicity could be obtained. Further, it was found that the complexity of analysis rapidly increased as more components were added. As a result, the possibility of using low power active components was investigated.

4.4 Active Compensation Technique

The recent introduction into the commercial market of micropower operational amplifiers designed for battery applications motivated the investigation of active techniques for synthesizing quadratic voltage versus temperature behavior. Further, because ultralinear temperature sensors (±0.1°C) over the temperature range specified were commercially available, a simple squaring or multiplication scheme was devised.

Figure 4.5 shows the circuit used to provide a quadratic voltage versus temperature signal. TL1 and TL2 are identical thermistor-resistor components which have a linear voltage-temperature response. Buffer amplifiers OA1 and OA3 provided a high impedance load to the thermistor networks. By using the linear voltage output from TL1 to drive TL2 with proper feedback from the output of potentiometer P3, a quadratic voltage-temperature curve was synthesized, as shown diagramatically in Fig. 4.5. Both the curvature of the quadratic function and temperature for minimum voltage can be controlled arbitrarily through P_1-P_3. Calibration was performed by replacing TL1 and TL2 with dummy resistors to simulate the appropriate output at different temperatures. Both the quadratic curvature and the minima temperature location were adjusted to give a least square fit with the calibration curve of phase shifter voltage versus temperature for constant frequency.

OA1-4 were micropower op amps and the total electronics drew only ½ mW of power from a 4 V supply, the majority of which was dissipated by the temperature sensors.

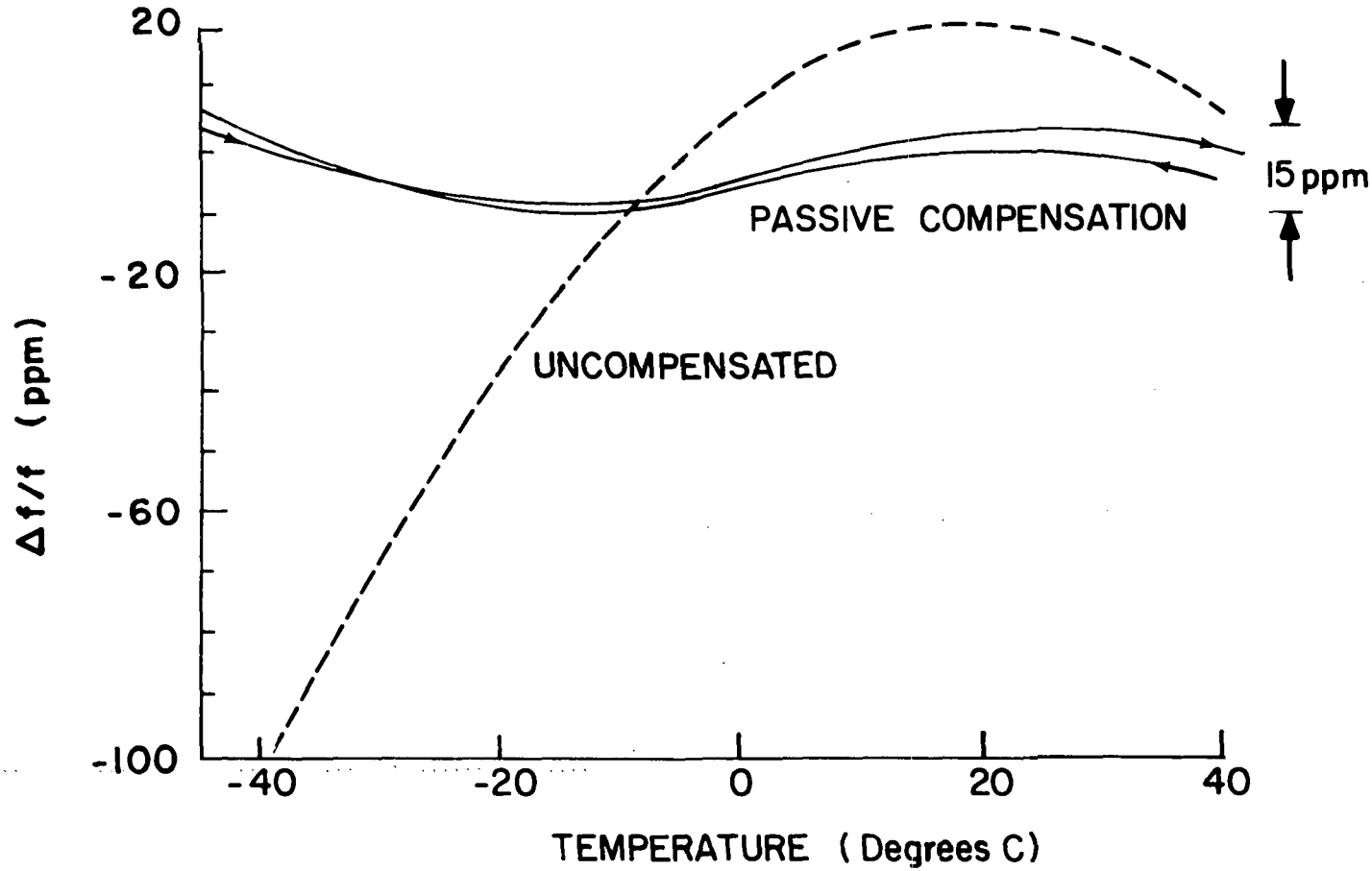

Figure 4.4 Comparison Between Uncompensated and Compensated Response Using Passive Compensation Circuit.

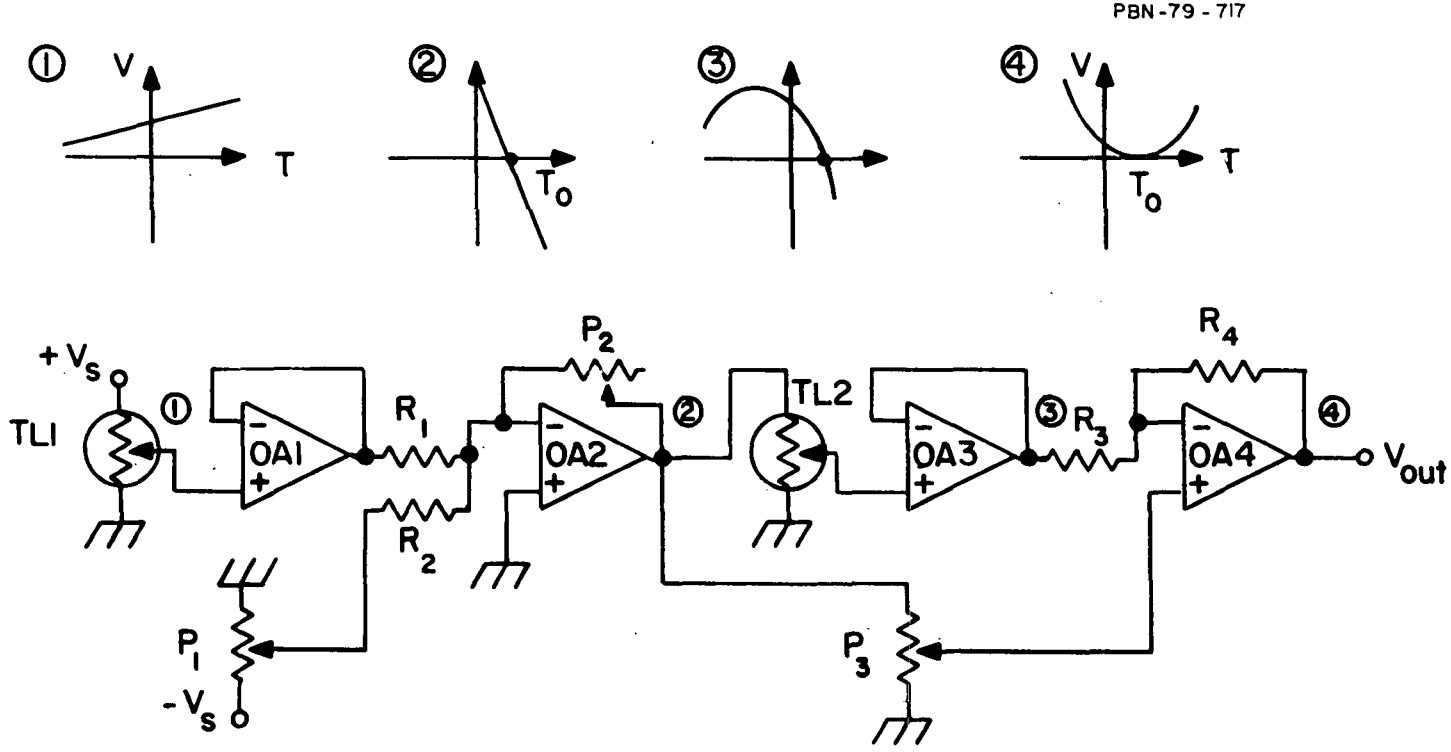

$R_1 = R_2 = R_3 = 100\ K\Omega$

$R_4 = 300\ K\Omega$

$P_1 = P_3 = 100\ K\Omega$

$P_2 = 200\ K\Omega$

OA1-OA4 = RCA CA3078 at Micropower OP Amp

$V_S = +2$ *Volts*

TL1, TL2 = YSI Thermolinear Component YS44211A

Figure 4.5 Low Power Active Compensation Circuit.

Figure 4.6 shows the actual compensated frequency response for a 1.6 μsec delay line with heating and cooling rates of about 1.5°C/min. Total frequency deviation including hysteresis is about 8 ppm. These errors are primarily due to undesired temperature-dependent phase shifts introduced by two components, the rf amplifiers and the voltage-controlled phase shifter.

4.5 Sources of Compensation Error

One of the primary sources of error in temperature compensation was a thermal hysteresis, evident in Figs. 4.2, 4.4, and 4.6. By temperature cycling the SAW delay line by itself with the remaining amplifier circuitry held at constant temperature, it was determined that the SAW device produced no hysteresis effects provided that it was mounted in a sealed evacuated or nitrogen back-filled package. One source of the hysteresis was determined to be the temperature dependence of the varactor diodes contained within the voltage-controlled phase shifter. These diodes, which behave electrically as voltage-controlled variable capacitors, are connected in a reflective hybrid coupler circuit[4.7] and produce a phase shift which is linearly proportional to the applied bias voltage. However, due to a temperature-dependent built-in junction potential, these diodes also produce a linear phase shift with temperature. The superposition of this linear phase shift component with the quadratic temperature dependence of the SAW device results in a temperature-shifted turnover point. Further, because the phase shifter is located apart from the SAW device, it thermally lags or leads the SAW upon cooling and heating by an amount ΔT_{LAG}. This results not only in a turnover point shifted downward in temperature by ΔT_o but also two slightly different minima shifted by $(\Delta\phi/\phi)_{SHIFT}$ as shown in Fig. 4.7. This apparent hysteresis can be minimized in theory by moving the phase shifter in closer proximity to the SAW device. However, because our off-the-shelf phase shifter was in a relatively large package, in practice this could not be done. The best solution seems to be to design a phase shifter operating at high bias voltages in order to reduce the temperature dependence of the varacter diodes.[4.8]

One of the most significant sources of unwanted phase shift for the oscillator circuit was the temperature-dependent phase shifts produced by our

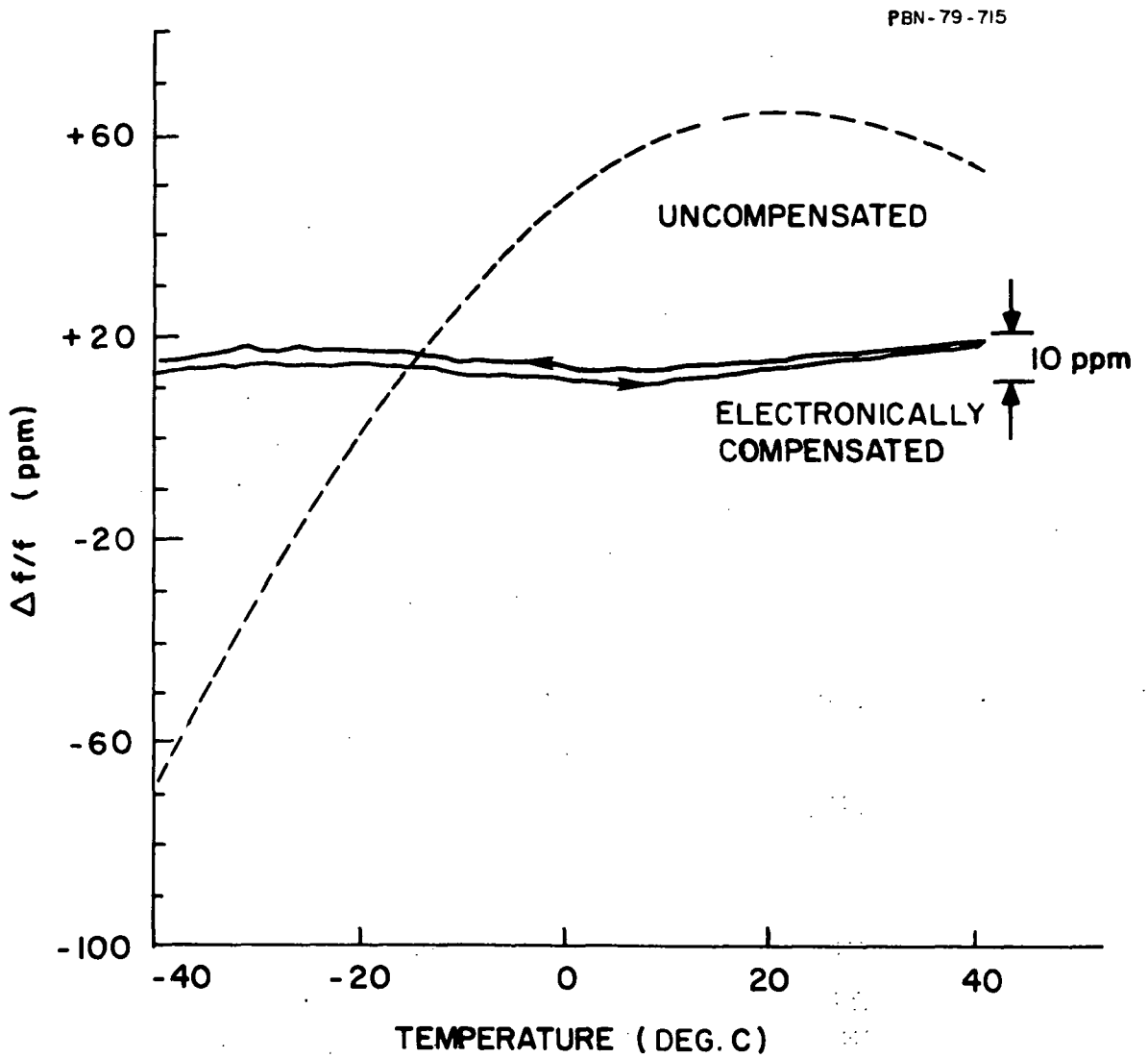

Figure 4.6 Comparison Between Uncompensated and Compensated Response Using Active Compensation Circuit.

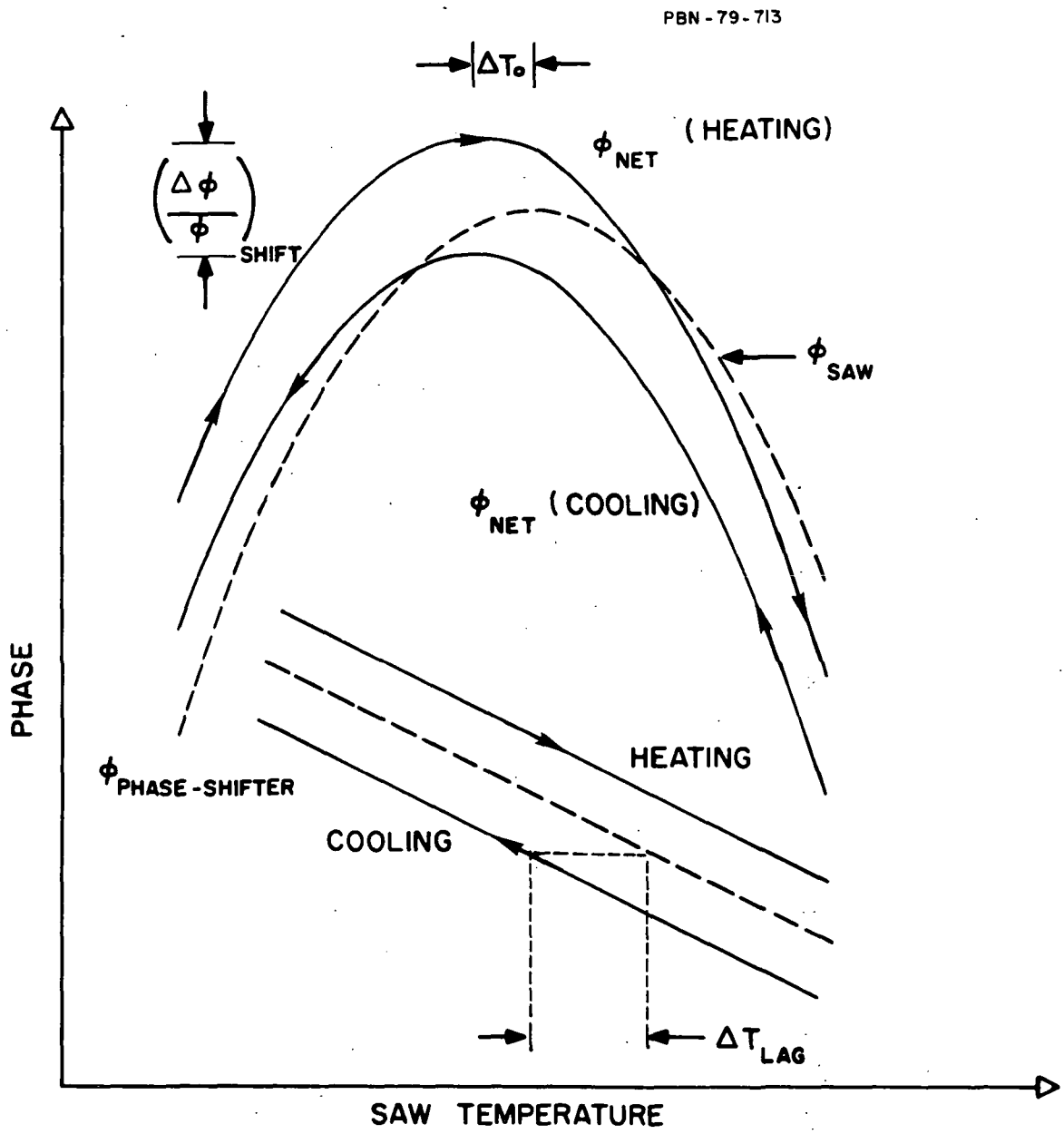

Figure 4.7 Phase Shifter Induced Thermal Hysteresis.

amplifiers. This phase shift exhibited two independent components. It was found that the amplifier gain saturation varied with temperature and that the net amplifier phase shift was a function of the amount of saturation. Empirically, we found that matching the amplifiers to 50 ohms minimized gain variation with temperature. In addition, there existed a gain-independent phase shift variation with temperature (Fig. 4.8) for a typical two-stage cascaded amplifier incorporated in our oscillator. The phase shift is seen to be rather linear with temperature below 20°C. In this temperature range the effect of the amplifier phase shift is similar to that discussed for the phase shifter. For higher temperatures, the deviation from linearity is large, the phase shift becoming temperature-insensitive around 35°C. The total result is not only to produce an apparent hysteresis in the quadratic phase-temperature curve but also to distort it. Though the source of the phase shift has not been determined, it may very well be due to temperature-dependent inductors or capacitors used in the amplifier matching circuitry. For sufficiently high frequency devices, tuning may be possible using either lumped-element air-core or printed-circuit inductors or stripline matching techniques to minimize phase shift dependence on temperature.

4.6 Conclusions

A significant improvement has been achieved in temperature stability through the use of temperature compensation. With an active circuit, the frequency variation was reduced to ±4 ppm (±1.6 KHz), while a passive circuit gave a variation of ±8 ppm (±3.2 KHz). The active circuit uses low-power operational amplifiers and consumes no more power than the passive circuit. The active circuit is much more flexible than the passive technique; therefore it gave better results. However, the extra cost of the amplifiers ($\sim$ \$10 per amplifier) makes the active approach a little more expensive.

The limiting characteristics of the compensation circuits have been identified and some improvement would be possible with further work. The rf amplifiers were identified as one source of error. Thus they would be an area of future effort. Further, the oscillator circuit should be laid out to minimize the thermal lag between the various components.

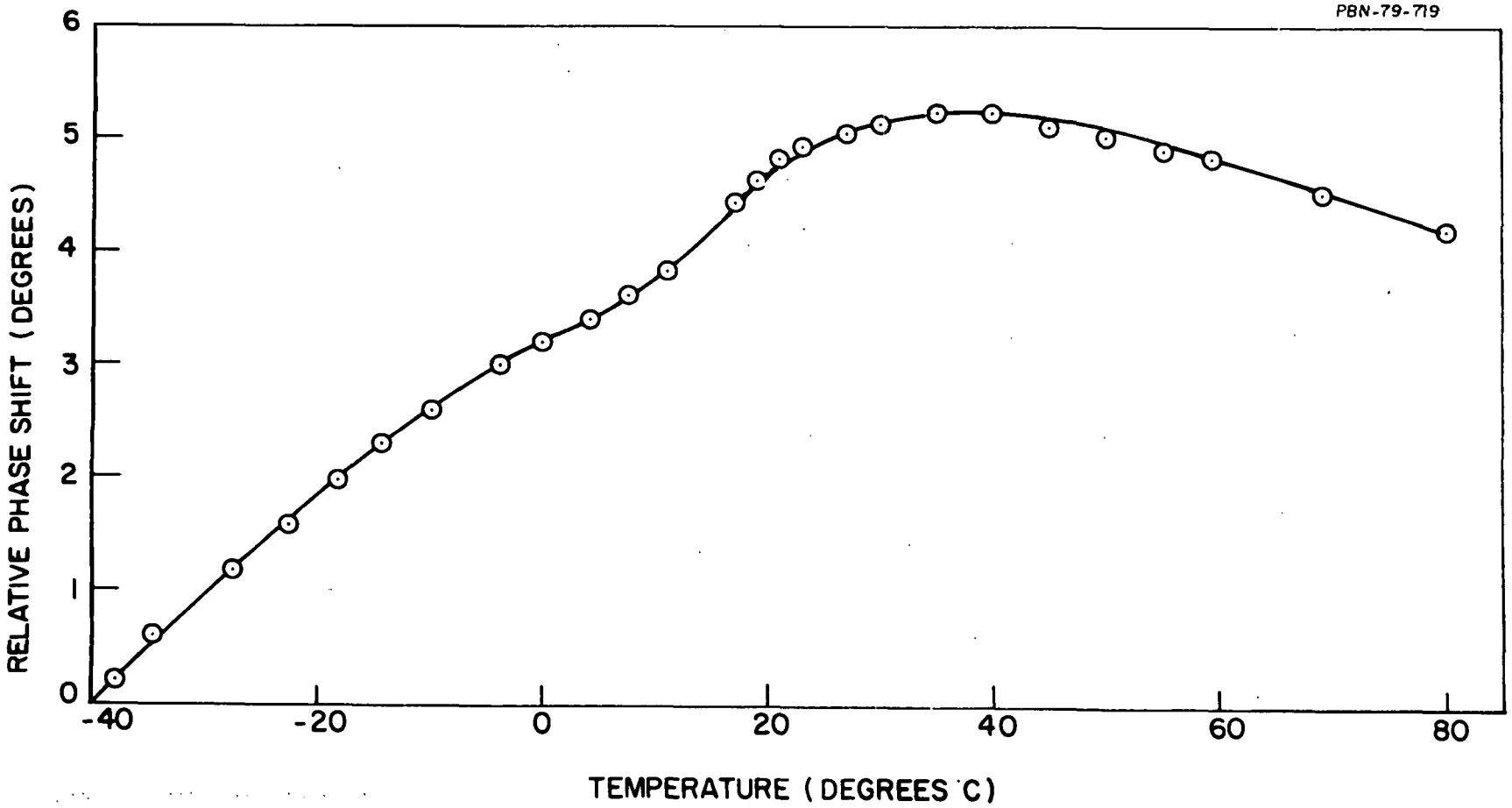

Figure 4.8 Measured Temperature Dependence of Phase Shift for High Gain rf Amplifiers.

The requirement for a frequency stability of 4.2 Hz in 15 minutes (0.28 Hz in 1 minute) also amounts to a temperature stability requirement. It is difficult to be very quantitative about this goal, since it is not clear what temperature change the oscillator will actually see in a 15-minute period. Clearly, if the oscillator were exposed to the maximum temperature change of 3°/min for the outside environment, the goal would not be met. However, it is not reasonable for the oscillator to actually see this large a temperature change, because of a thermal time lag between the outside environment and the inside of an electronic package.

A crude thermal analysis was made to estimate just how well insulated the oscillator would have to be to meet the desired stability of 0.28 Hz ($\sim$ 7 parts in 10^{10}) in 1 minute. It was assumed, in this analysis, that the outside temperature varied at the maximum rate of 3°C/minute and that the maximum temperature coefficient of the oscillator was 0.5 ppm/°C (See Fig. 4.6). From these assumptions it was determined that a thermal time constant of $\sim$ 2 days would be required to reduce the temperature change in one minute to $\sim$0.001°C, which would give the desired frequency stability. A time constant of 2 days appears to be possible with reasonable values for insulating capacity and thermal mass, but the necessary warmup time may be excessively long.

Though it is not clear that the desired stability of 0.28 Hz per minute can be met in a real system for the assumptions made above, the numbers suggest that a stability approaching the desired value could be achieved in a somewhat more moderate environment.

REFERENCES

4-1. J. F. Dias, H. E. Karrer, J. A. Kusters, J. H. Matsinger, M. B. Schulz, "Temperature Coefficient of Delay-Time for X-Propagating Acoustic Surface Waves on Rotated Y-Cuts of Alpha Quartz," IEEE Trans. Sonics and Ultrasonics, SU-22, p. 46, 1975.

4-2. H. A. Batdorf, "Temperature-Compensated Crystal-Controlled Oscillators Operating from 800 KHz to 1500 KHz," Proc. 23rd Symposium on Frequency Control, 192, 1969.

4-3. D. L. Thomann, "A Microcircuit Temperature Compensated Crystal Oscillator (MCTCXO)," Proc. 28th Symposium on Frequency Control, 214, 1974.

4-4. D. E. Newall, H. Hinnah, "A Report on TCXO's and Segmented Compensation," Proc. 23rd Symposium on Frequency Control, 187, 1969.

4-5. P. C. Duckett, R. J. Peduto, G. V. Chizak, "Temperature Compensated Crystal Oscillators," Proc. 24th Symposium on Frequency Control, 191, 1970.

4-6. S. Schobowski, "A New Approach to a High Stability Temperature Compensated Crystal Oscillator," Proc. 24th Symposium on Frequency Control, 200, 1970.

4-7. R. Fekete, "Varactors in Voltage Tuning Applications," Microwave Journal, 53, 1964.

4-8. Alpha Industries Inc., Application note #80500.

5.0 TASK III - HIGH EFFICIENCY AMPLIFIER

5.1 Introduction

For the aging and temperature compensation experiments, commerical wideband amplifiers were used in the oscillators. These amplifiers are very versatile because of their large bandwidth and relatively stable gain and phase shift. However, for battery powered applications where power consumption is of great concern, these amplifiers are not well suited because of their low efficiency. The commercial amplifiers range in efficiency from less than 0.1 percent to 6 percent, with the higher powered amplifiers giving the highest efficiency.

Another important factor is the available gain, which determine what fraction of the power can be coupled out. This can be seen in the amplifier configuration used for the aging studies (Fig. 3.2). The cascaded UTO 502 and 503 provide an rf output power of about 25 mW with a gain of 22 dB and a dc power consumption of 1.75 watts (73 ma at 24 Vdc). The amplifier efficiency is 1.4 percent, but normally a 10 dB coupler was used for the output. This gives an oscillator efficiency of 0.14 percent. With relatively minor changes in the circuit a 3 dB coupler could be used to increase the oscillator efficiency to 0.7 percent. However, even under ideal conditions, the best oscillator efficiency that could be achieved with commercial amplifiers would be about 3 percent. Under these conditions, the dc power is too high for most battery applications, therefore a new high-efficiency amplifier design was considered.

The desired characteristics of a new amplifier are high dc to rf efficiency and sufficient gain to allow a significant fraction of the power to be coupled out. Specifically, design goals of at least 25 dB gain and a minimum of 25 mW rf output were chosen. DC requirements were set at not more than 8 volts and minimum current.

High efficiency is not possible with a class A amplifier, so nonlinear operation must be used. Class C amplifiers can give high efficiency, but

they tend to have low gain and therefore are not suitable for this oscillator application. Consequently, an amplifier design operating in a switching mode was chosen. In switch mode operation, the voltage across the active device appears as a square wave, and current flows through the device only when the voltage is at or near zero. Thus, the power dissipated in the amplifier is very low.

To achieve switch mode operation the active device must be able to generate a square wave, so it must have good high frequency response up to about the 9th harmonic. This is not too difficult at low frequencies, but at 401 MHz a good high frequency transistor must be used. Further, we must use a tuned circuit which can present a high load impedance to the amplifying devices at a high frequency, with its odd harmonics. Such a tuned circuit happens to be a shorted one-quarter wavelength transmission line.

The impedance of a shorted transmission line can be expressed as follows:

$$Z = j \tan\left(\frac{2\pi f \ell}{v}\right) \qquad (5\text{-}1)$$

where

f = frequency, in Hz
ℓ = length of line
v = propagation velocity of the line.

Whenever the quantity in parentheses becomes $\pi/2$ or any odd multiple of $\pi/2$, the impedance becomes infinite. In an amplifier circuit, the use of the quarterwave shorted line by itself is not enough — the tuned circuit must also remove the reactive loading effects of the device's output capacitance and any lead or bonding wire inductance. To achieve this requirement, the transmission line becomes shorter than the quarter wavelength.

To evaluate the use of a switch mode amplifier in a SAW oscillator, we constructed three oscillators; two, which were identical, used dual gate GaAs field effect transistors (FET's), while a third used a silicon dual gate

FET. The use of dual gate FET's provides sufficient gain to allow for coupling out a significant fraction of the signal. Since the best electrical performance was achieved with the GaAs FET amplifiers, these will be discussed first.

5.2 GaAs FET (Raytheon LND 832) Oscillator

The GaAs FET is a high frequency device with significant gain up to frequencies in excess of 10 GHz. Thus it is ideal for switch-mode operation. Also, now that dual gate GaAs FET's are becoming available, high enough gain can be obtained to design a high efficiency oscillator. Figure 5.1 shows the design that was used to construct two high efficiency oscillators using the same aluminum SAW lines that were used in the other tasks.

In Fig. 5.1, the line lengths, lines 1 and 2, constitute the shorted transmission line; C_6 is a dc blocking capacitor, and L_4 supplies the drain voltage, V_{dd}, to the FET, Q_1, through line 1. Q_1 was found to have approximately 1 pf of output capacitance, which represents a fairly low capacitive reactance compared with the 1,000-ohm desired load resistance of the amplifier at the operating frequency, as shown in Table 5-1.

To counter the effect of capacitive loading on Q_1 output, the line lengths of lines 1 and 2 must be reduced to present a 398-ohm inductive resistance, less the inductive reactance of the Q_1 bonding wire, which is approximately 1 nanohenry, L_A. However, by adjusting the line length for optimum reactance cancellation at the 9th harmonic (3600 MHz), good results are obtained at all the odd harmonics (see Table 5-1). Thus, this tuned circuit could sustain a square waveform at 400 MHz. The resulting line length was 82.6 electrical degrees.

To match the 50 Ω load impedance at the oscillator output to the amplifying device, it is first necessary to determine the desired power output. For a 50-mW output and an 8-V drain supply (Fig. 5.1), a load resistance to be reflected to the amplifying device, Q_1, is calculated in equations (5-2) and (5-3).

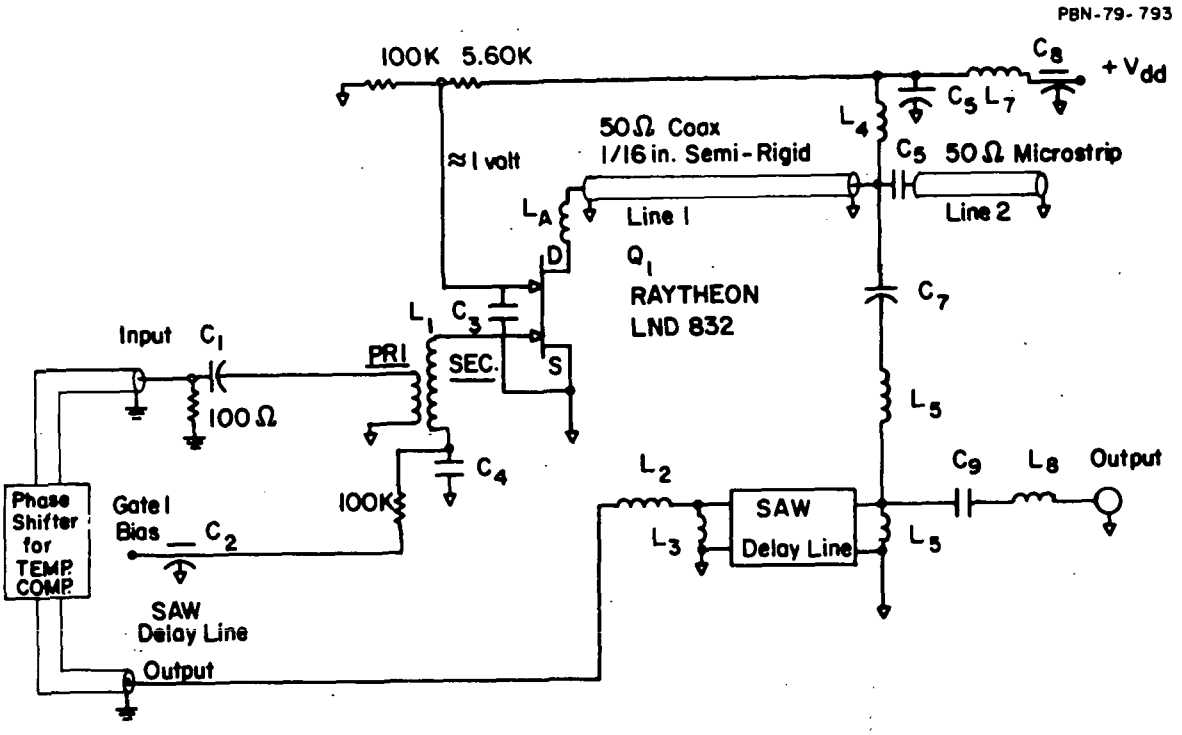

C_1 - 7 pF NPO

C_2 - .01 μF Feedthrough

C_3 - 100 pF chip; mounted on the LND-832 chip carrier

C_4 - .1 μF chip

C_5 - .1 μF chip

C_6 - .1 μF chip

C_7 - 2.2 pF NPO

C_8 - .01 μF Feedthrough

C_9 - 4.7 pF NPO

Line 1, Line 2 } SEE TEXT

L_A - See Text

L_1 - SEC 150 NHY (about 7 Turns #20 on 3 mm form)

PRI - 1 Turn #14 Close to Center of SEC.

L_2 - 130 NHY (6 Turns #18 on 3 mm diameter)

L_3 - 23.2 NHY (2 Turns #18 on 3 mm diameter)

L_4 - 400 NHY rf choke (10 Turns #30 on 3 mm diameter)

L_5 - 80 NHY 5 Turns #18 on 3 mm diameter

Figure 5.1 Schematic of Oscillator Using LND 832 Dual-Gate FET.

TABLE 5-1

Frequency MHz	Capacitive Reactance of 1 pf (Ω)	Inductive Reactances Of Line 1 + Line 2Ω*	Of LA (1 nh)
400	398	385	2.5
1200	133	122	7.5
2000	79.6	66.3	12.5
2800	56.8	39.3	17.5
3600	44.2	21.6	22.5

Resulting Reactive Loading on Amplifying Device, Q_1

Frequency MHz	Reactive Impedance (Ω)
400	14.3 K
1200	5.76 K
2000	6.2 K
2800	31.8 K
3600	3.8×10^{11}*

* *The line length (line 1 + line 2) is adjusted for resonance at the 9th harmonic (3600 MHz). Line length was 82.6 electrical degrees.*

$$P_{out} = \frac{(Vdd)^2}{R_L} \tag{5-2}$$

$$R_L = \frac{Vdd^2}{P\ (out)}$$

$$= \frac{(8)^2}{50 \times 10^{-3}} = 1.28\ K\Omega \tag{5-3}$$

Since the load at the oscillator output is 50 Ω, a voltage step-down ratio is required:

$$\frac{V_{out}}{V_{load}} = \sqrt{\frac{50}{R_L}} \cong 0.198 \tag{5-4}$$

This is most conveniently done by tapping off the required voltage from the shorted delay line, as shown in Fig. 5.1. The position of the tap should be so chosen according to equation (5-5):

$$V(x) = V_{in} \frac{\mathrm{Sin}\left(\frac{2\pi fx}{v}\right)}{\mathrm{Sin}\left(\frac{2\pi f\ell}{V}\right)} \tag{5-5}$$

$$0.198 = \frac{\mathrm{Sin}\ (Z)}{\mathrm{Sin}\ (82.6°)} \tag{5-6}$$

$$X = \mathrm{Sin}^{-1}\ (0.198 \sin 82.6°)$$

$$= 11.3 \text{ electrical degrees}$$

where

V_{in} = input voltage to the shorted line
X = distance from shorted end of line
ℓ = total length of line
v = velocity of propagation in line

Thus, the tap should be approximately 1/8 of the line length from the shorted end. This is the length of line 2; line 1 comprises the balance of the line length required to make up the 82.6 electrical degrees. A series resonant circuit C7-L5 is added to the tap to reject the higher harmonics.

Impedance matching to the amplifier input and SAW line follows the usual methods used for a single frequency impedance transformation. The driven end of the SAW line is not matched to any particular impedance; only L_6 is added to tune out the line capacitance. The result is a 500-ohm loading across the amplifier output, thus absorbing about 10 percent of the amplifier power output. A series resonant circuit L8-C9 was added to further suppress harmonics in the output.

The electrical performance of the two GaAs FET amplifiers was outstanding, as shown below.

	Breadboard 1	Breadboard 2	
Gain (*As an Amplifier*)	25 dB	26 dB	
Bandwidth (*As an Amplifier*)	50 MHz	35 MHz	
Power Input (volts × ma)	7.9 V × 11.5 ma	8.0 V × 17.5 ma	5.8 V × 9.7 ma
Power Output (mW)	40 mW	56 mW	25 mW
Efficiency	0.438	0.400	0.444

The rf output power ranged from 25 mW to 56 mW for dc voltages as low as 5.8 V. With a dc to rf efficiency as high as 44 percent, the goals and requirements as stated previously were met.

Unfortunately, when the frequency stability of the oscillators was evaluated, it was found to be degraded over that observed for oscillators using commercial wide band amplifiers. Gate 1 of the FET is a reverse biased Schottky barrier diode and therefore has a voltage dependent capacitance. Since the gate capacitance is part of the tuned circuit which provides the input impedance matching, a voltage dependent phase shift is present. This phase shift is directly responsible for the voltage dependence of the frequency shown in Fig. 5.2. For low values of V_{dd}, the frequency is particularly sensitive to the gate voltage V_g.

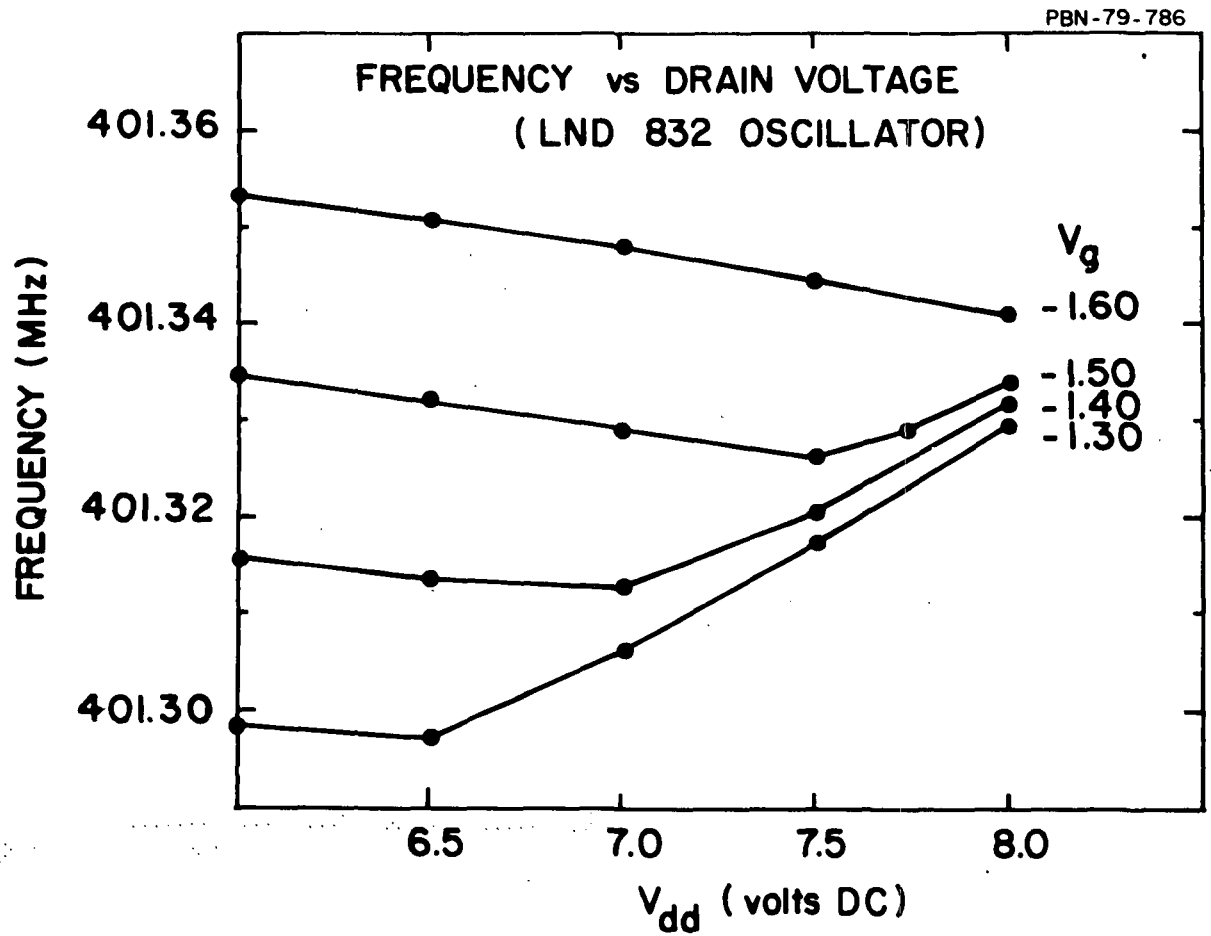

Figure 5.2 Dependence of GaAs FET Oscillator Frequency on Drain Voltage, V_{dd}, for Several Values of Gate Voltage, V_g.

An attempt was made to measure the temperature dependence of the frequency for these oscillators, but so many small, irregular jumps in frequency occurred that it was impossible to locate the turnover point. The basic parabolic temperature dependence appeared to be there, but the turnover point could not be localized to better than about ± 20°C. It appears that these frequency stabilities are also related to phase shifts caused by small changes in the gate capacitance.

The short term frequency stability of an oscillator using a GaAs FET was measured to be 8×10^{-9}; it also was observed to be somewhat dependent on V_g and V_{dd}. This is nearly a factor of ten larger than that observed for oscillators using commercial amplifiers.

5.3 Silicon FET (Signetics SD-303) Oscillator

The oscillator built with a silicon dual gate FET showed much better frequency stability, but its electrical parameters were not nearly as good as the GaAs FET oscillators. The design for this oscillators is shown in Fig. 5.3. It is very similar to the design in Fig. 5.1, in that lines 1 and 2 serve the same purpose in impedance matching the output load to the amplifier. Lines 3 and 4 are also for impedance matching purposes, only in this case they transform the impedance of the SAW line to 50 Ω.

The electrical characteristics of this oscillator are listed below.

Gain (*As an Amplifier*)	18 dB	
Bandwidth (*As an Amplifier*)	35 MHz	
Power input (volt × ma)	15V × 14.8 ma	9V × 5.5 ma
Power output (mW)	20 mW	2 mW
Efficiency	0.09	0.04

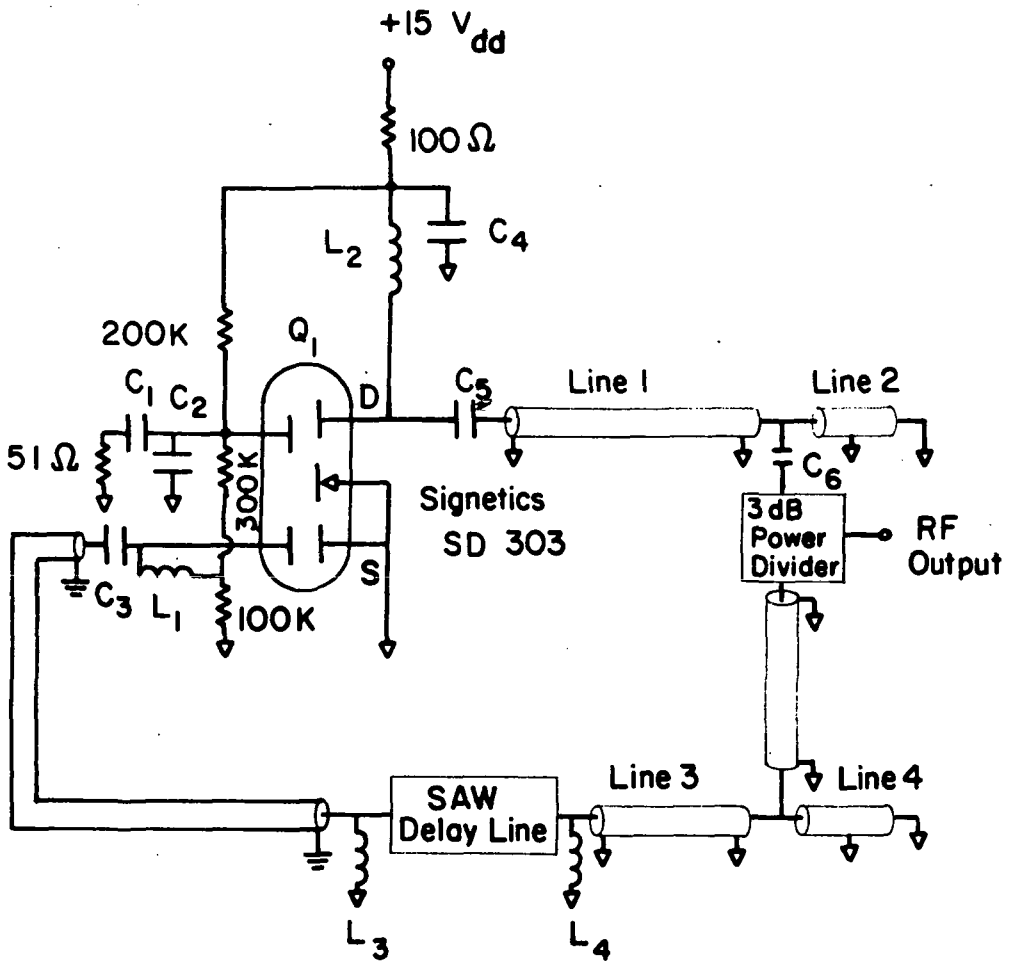

C_1	-	390 pF	L_1	-	3 turns, 6 mm diameter
C_2	-	390 pF	L_2	-	7 turns, 6 mm diameter
C_3	-	7 pF	L_3	-	1 turn, 10 mm diameter
C_4	-	0.1 μF	L_4	-	1 turn, 25 mm diameter
C_5	-	7 pF			
C_6	-	7 pF	Lines 1-4 - See Text		

Figure 5.3 Schematic of Oscillator Using SD 303 Dual-Gate FET.

Part of the reason for the lower efficiency is that only 50 percent of the power could be coupled out because of the limited gain that was available. However, even considering this, the efficiency of the silicon FET amplifier was not as good as that of the GaAs FET amplifiers, and it also required a higher operating voltage.

The main advantage of the silicon FET oscillator is its much better frequency stability. Figure 5.4 shows the dependence of frequency on dc voltage for this oscillator. It is roughly an order of magnitude better than the GaAs FET oscillator and essentially equivalent to the stability of commercial amplifier. The main reason for this increased stability is that the silicon FET has an insulated gate whose capacitance is not voltage dependent. The insulated gate, however, contributes to a reduced gain at high frequencies and hence to a lower efficiency.

The temperature dependence of the frequency was measured and the amplifier was observed to shift the turnover point upwards by about 5°C. This is comparable in magnitude but opposite in sizes to that observed for commercial amplifiers. The short term stability of the silicon FET oscillator was measured as 7×10^{-10}, which was the same value as observed when the SAW line from the silicon FET was operated with a commercial amplifiers. Due to the breadboard construction of the silicon FET oscillator, its frequency was sensitive to mechanical vibration, but this could be eliminated with an improved circuit board and more stable mounting of components.

The silicon FET amplifier has one other advantage. At $1 each, the SD-303 is considerably less expensive than the LND832, which costs $100 each. However, the cost of GaAs FET's will drop substantially in the future.

5.4 Conclusions

Operation of the silicon FET oscillator has demonstrated that a substantial improvement in efficiency can be obtained without degrading frequency stability. However, the very high efficiency of the GaAs FET oscillator was

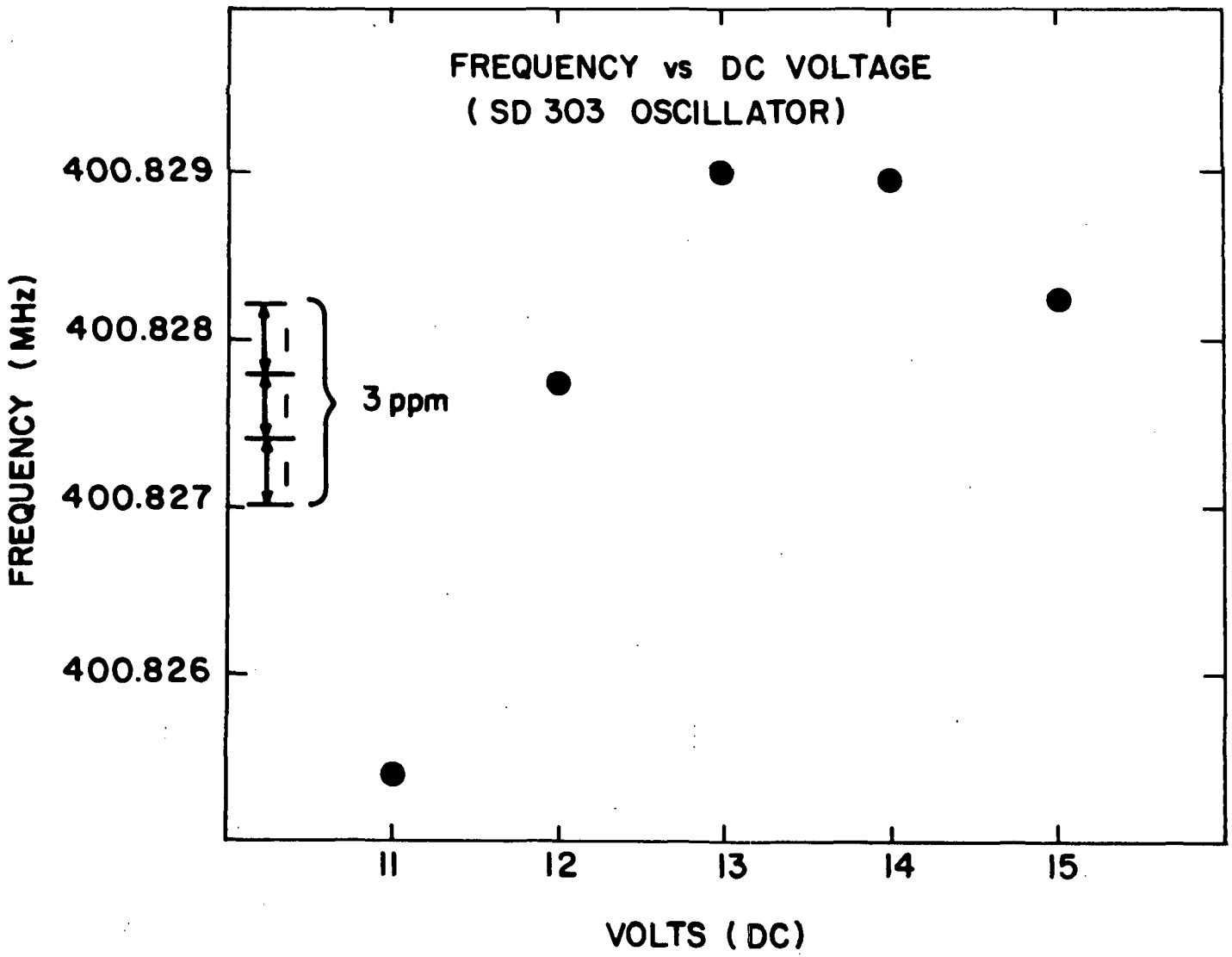

Figure 5.4 Dependence of Silicon FET Oscillator Frequency on Voltage from dc Power Supply.

obtained at the price of a substantial degradation in stability. The dual gate GaAs FET is a very recent development, and further improvements in FET technology may influence the stability problem. The LND832's used in this program were supplied in chip form and were operated in an unsealed environment. Therefore, it is possible that surface contaminations may have contributed to some of the problems. Future designs should include proper packaging for the FET.

6.0 TASK IV - SHOCK AND VIBRATION TESTS

6.1 Specified Tests

In order to determine the survivability of SAW oscillators in a realistic environment, it was necessary to test them under shock and vibration. Specifically, MIL-STD-202 was used as stated in Sec. 1.2. For shock testing, Method 213 was followed for half-sine shock pulses up to the specified 100 G's. The vibration test followed Method 201, which requires a sinusoidal displacement of ± 0.03 in. for frequencies from 10 to 55 Hz.

6.2 Test Devices

The shock and vibration tests were performed on four SAW oscillators which represented three different mounting techniques for the SAW substrates. One of the devices was mounted in an HC36/U cold weld enclosure, as shown in Fig. 3.1. Two other devices were mounted in flatpacks with 0.010 in. gold wire straps as shown in Fig. 6.1. This is the packaging technique that was used in the first part of this program. As discussed earlier, the flatpack has not been found to be particularly good for low aging, but primarily the strapdown technique was being tested, since it could also be used in other package types such as the TO8. Finally, the third mounting technique used a spring clip and adhesive arrangement, as shown in Fig. 6.2. This last technique has the potential for being fabricated in a more reproducible manner than the gold wire straps and may also eliminate some of the small irregular frequency jumps seen in the aging and temperature dependence of strap-mounted devices. The adhesive is a special polyimide compound (Ablebond 71-1) which can withstand very high temperatures (500°C) and outgases very little when properly cured. The polyimide adhesive has been found to be useful in low aging quartz crystal resonators.

6.3 Results of Tests

Before the start of the shock and vibration tests, the frequency, short-term stability, and power output of each of the four test oscillators were measured. After each stage of the test, the frequency was measured again.

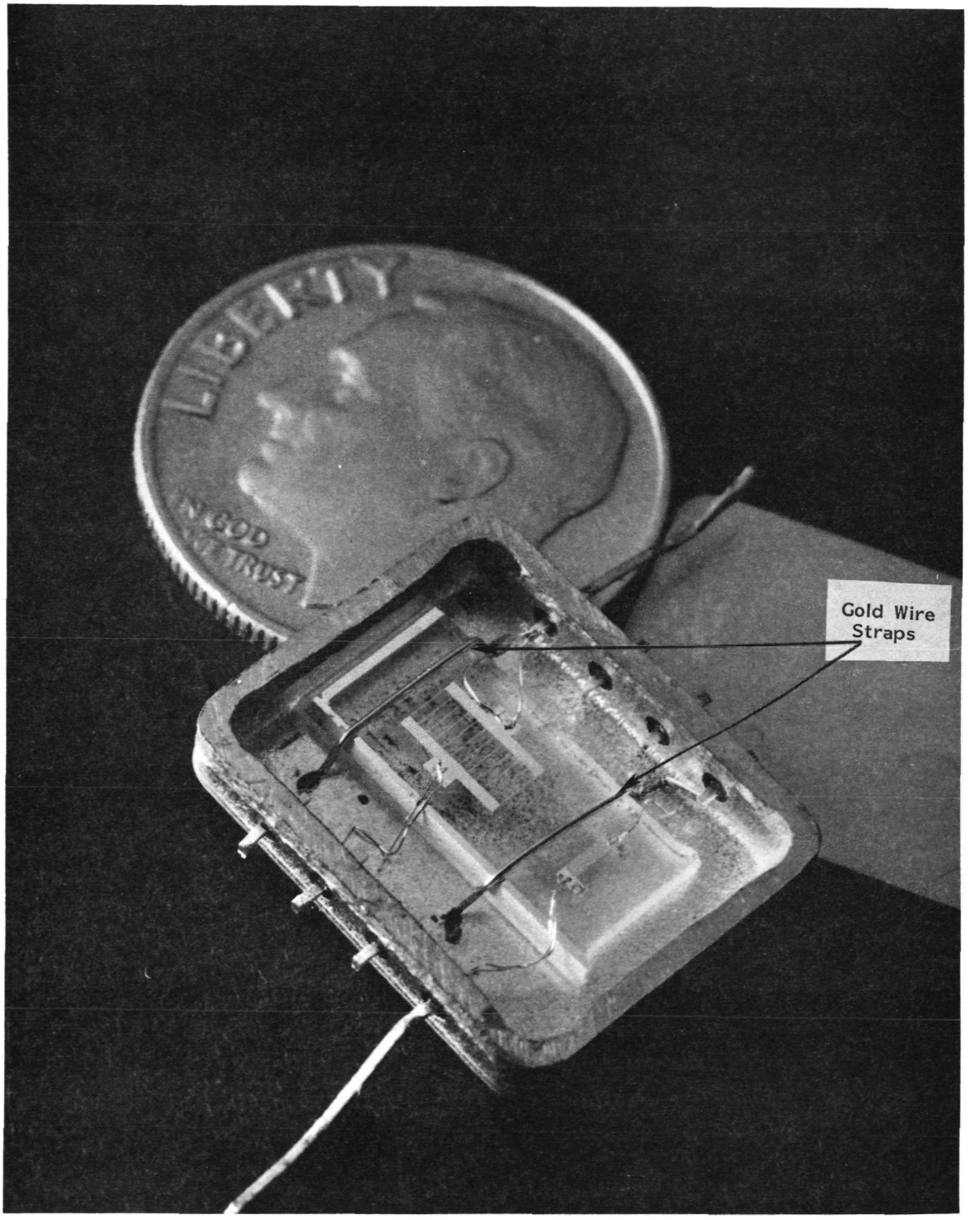

Figure 6.1 SAW Device Mounted in a Flatpack.

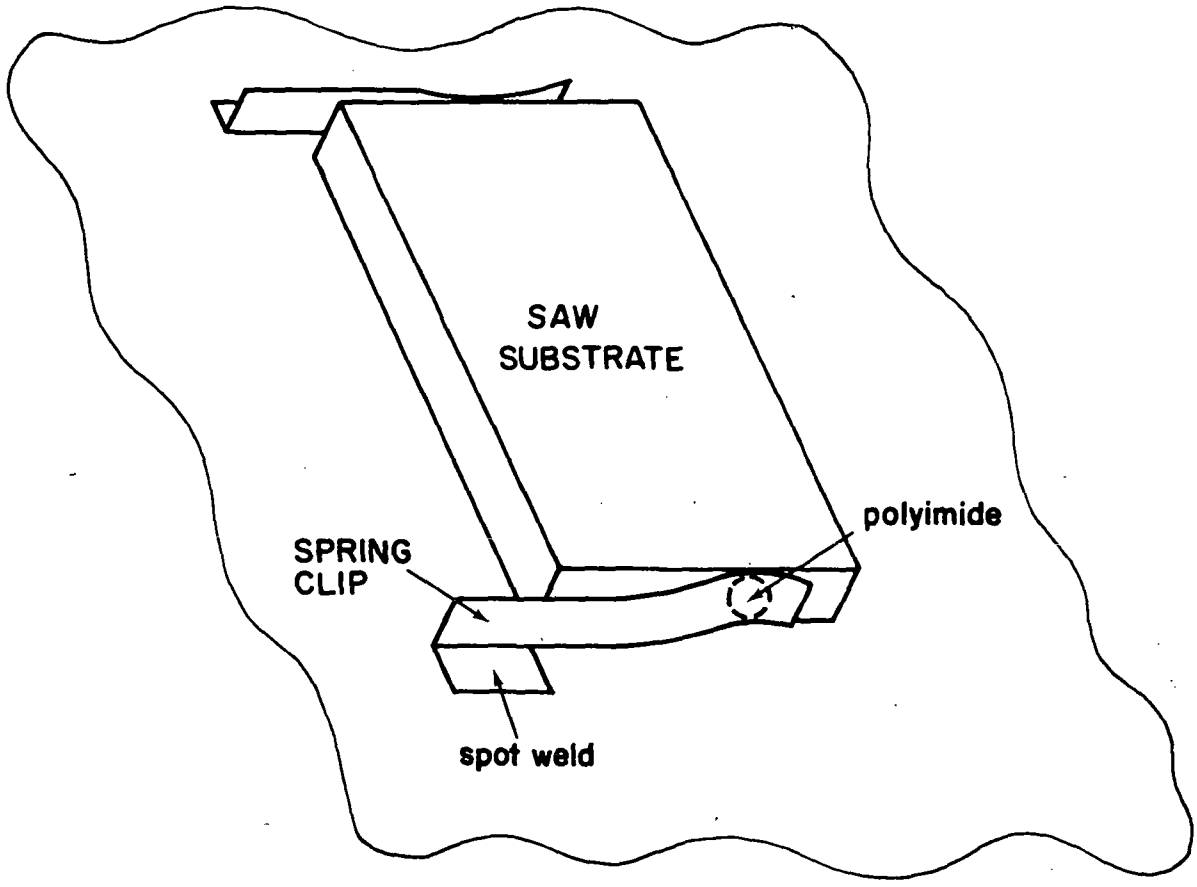

Figure 6.2 Illustration of Mounting Technique Using Spring Clips and Polyimide Adhesive.

The first stage in the test was vibration from 10 to 55 Hz. The displacement was ±0.030 in., and the frequency was swept from 10 to 55 Hz in one minute. The vibration was applied for two hours to each of the three axes. After vibration along each axis, the frequency of each oscillator was measured; throughout this stage no deviation greater than ±3 ppm (±1200 Hz) was observed.

The next stage involved 100 G shock pulses applied in both directions, along each of the three axes. Three pulses of 6 msec duration were applied in each direction. Again, no deviation greater than ±3 ppm was observed. Since no problems had been encountered up to this point, the shock levels were increased. The following half-sine pulses were applied three times in both directions for each of the three axes:

1.	150 G's	6 msec duration
2.	200 G's	5 msec duration
3.	500 G's	1 msec duration

Again, no significant change in frequency was observed.

Since all of the devices were still functioning satisfactorily, it was decided to perform more vibration tests at increasing levels until something failed. The additional vibration tests were somewhat different from the original tests in that a random vibration was used. In these tests, vibration frequencies from 20 Hz to 2000 Hz were applied simultaneously at a uniform acceleration level (white noise). The test devices were vibrated for fifteen minutes on each axis at an RMS level of 10 G's, and again no change in operation was observed. However, when the acceleration level was boosted to 20 G's RMS, one device ceased operating entirely and one became intermittent. At this point the tests were stopped.

The problem with the device that failed completely (goldwire straps in flatpack) was that an electrical lead connecting a transducer busbar to a pin on the flatpack came loose. In fact, it was observed that the strength of all the transducer bonds was relatively low on this particular device. This is characteristic of a device which has poor adhesion between the aluminum metallization and the quartz surface. Poor adhesion is usually a result of a slight contamination of the quartz surface before the metal is deposited. More careful attention to cleanliness or very thin layers of chrome or titanium under the aluminum can eliminate the problem. None of the other devices showed this kind of problem.

The oscillator that showed intermittent operation was the one with the HC36/U package and the problem was traced to either the SAW device or the package. The intermittence appeared to be sensitive to temperature changes, but the problem eventually disappeared before the specific cause could be identified.

The two oscillators that were still working after the final vibration tests showed no significant change in frequency, short-term stability, or output power level.

6.4 Conclusions

The shock and vibration tests showed that all three mounting techniques are very robust. None of the devices failed until moderately severe vibration levels were reached, and even then the failure mechanisms did not appear to be related to the mounting of the substrate.

7.0 CONCLUSIONS

A significant improvement in SAW oscillator performance has been demonstrated in this program. Reduced aging and temperature dependence have been obtained and oscillator circuits with increased efficiency have been built and demonstrated. Further, the survivability of SAW oscillators under severe shock and vibration has been demonstrated.

Oscillators have been built with an output power of at least 25 mW at 401.2 MHz with a short-term frequency stability of 1×10^{-9}. With demonstrated aging less than 5 ppm in 35 weeks and temperature stability of ±4 ppm (-40°C to +45°C), we have shown that SAW oscillators can stay within the ± 6 KHz (± 15 ppm) window specified in Sec. 1.2. This improved performance has been obtained through the use of temperature compensation circuits and high quality packaging techniques for the SAW devices. The temperature compensation circuit provides better than an order of magnitude improvement over uncompensated oscillator, while the cold weld packaging technique and preaging have reduced the long-term frequency drift from 10 - 15 ppm to well under 5 ppm.

The temperature compensation technique has greatly improved the likelihood of demonstrating a frequency stability of 4.2 Hz over 15 minutes. Clearly, the difficulty in reaching this goal depends on the temperature change observed by the oscillator over the 15 minute period; and with temperature compensation the required thermal isolation comes into the realm of realistic values.

For battery operated applications a high dc to rf efficiency is desired to extend the battery life for as long as possible. For this reason, 3 high efficiency amplifiers were built and tested. Circuits using a dual-gate GaAs FET exhibited an rf output at 401 MHz of more than 25 mW with an efficiency of 44 percent. Unfortunately, the GaAs amplifier significantly degraded the frequency stability. Good frequency stability was obtained with a circuit using a dual-gate silicon FET, but the dc to rf efficiency was only 9 percent.

Shock and vibration tests were performed on four oscillators and the results clearly demonstrate that no damage or change in frequency was observed until moderately severe vibration levels (somewhat higher than that in an airborn missile) were reached. Shock pulses up to 500 G's caused no damage or change in frequency.

Though a significant improvement in oscillator performance was achieved during this program, there are still areas where further improvement is possible. The low aging of the device preaged at 200°C strongly suggests that even further reduction in aging is possible. Further, the poor frequency stability of the GaAs oscillator can very likely be improved through the choice of a different type of FET or changes in the amplifier circuit. Finally, the individual achievements of low aging, temperature compensation, and high efficiency need to be combined into one oscillator that exhibits all of these desirable features.

S-2604A

SURFACE ACOUSTIC WAVE STABILIZED OSCILLATORS

Additional Aging Results

Raytheon Research Division
28 Seyon Street
Waltham, Massachusetts 02154

March 3, 1980

Addendum to Final Report for NAS5-25117

Prepared for:

Goddard Space Flight Center
Greenbelt, Maryland 20771

This report is a supplement to NASA final report NAS5-23701 and presents the results of an additional 27 weeks of aging tests for nine of the oscillators discussed in the final report. Figures 1, 2, and 3 of this report correspond to Figs. 3.3, 3.4, and 3.5 of the final report, except that the new aging data has been added. Overall, the new data is consistent with the previous results and none of the conclusions of the final report have been changed.

In Fig. 1, new data has been added to five of the six curves (Oscillator 1 is an older device and has not been operating). The trends observed during the first 35 weeks of operation, which were discussed in the final report, have generally continued. Oscillators 2 and 4 have aged upwards, although Oscillator 4 has shown a slight negative drift for the last 30 weeks. Oscillator 5 has shown a downward aging for virtually the whole time. Oscillators 3 and 6 have shown the lowest aging of all and, except for a downward kink on Oscillator 3 at about week 42, both have been consistently good from the beginning. The aging of Oscillator 6 is particularly interesting, since this device was baked at 200°C for seven days.

An additional 27 weeks of data has been added to all three curves on Fig. 2. The new data for all three oscillators is consistent with the earlier results and all trends have continued. Oscillator 7 holds the record for the least aging over the longest period of time.

In Fig. 3, data has only been added to the curve for Oscillator 16. As with most of the other oscillators, the new data for Oscillator 16 is consistent with the earlier data.

These aging tests have demonstrated that SAW oscillators with good long-term stability can be produced. Drift of less than 1 ppm in 93 weeks has been observed. In general the devices sealed in a coldweld enclosure (HC36/u) have done better than those sealed in flatpacks, but this may be due partly to the longer period of time between fabrication and testing of the coldweld devices. As discussed in the final report, this investigation has been very useful in beginning to identify the mechanisms that can cause long-term drift in SAW oscillators.

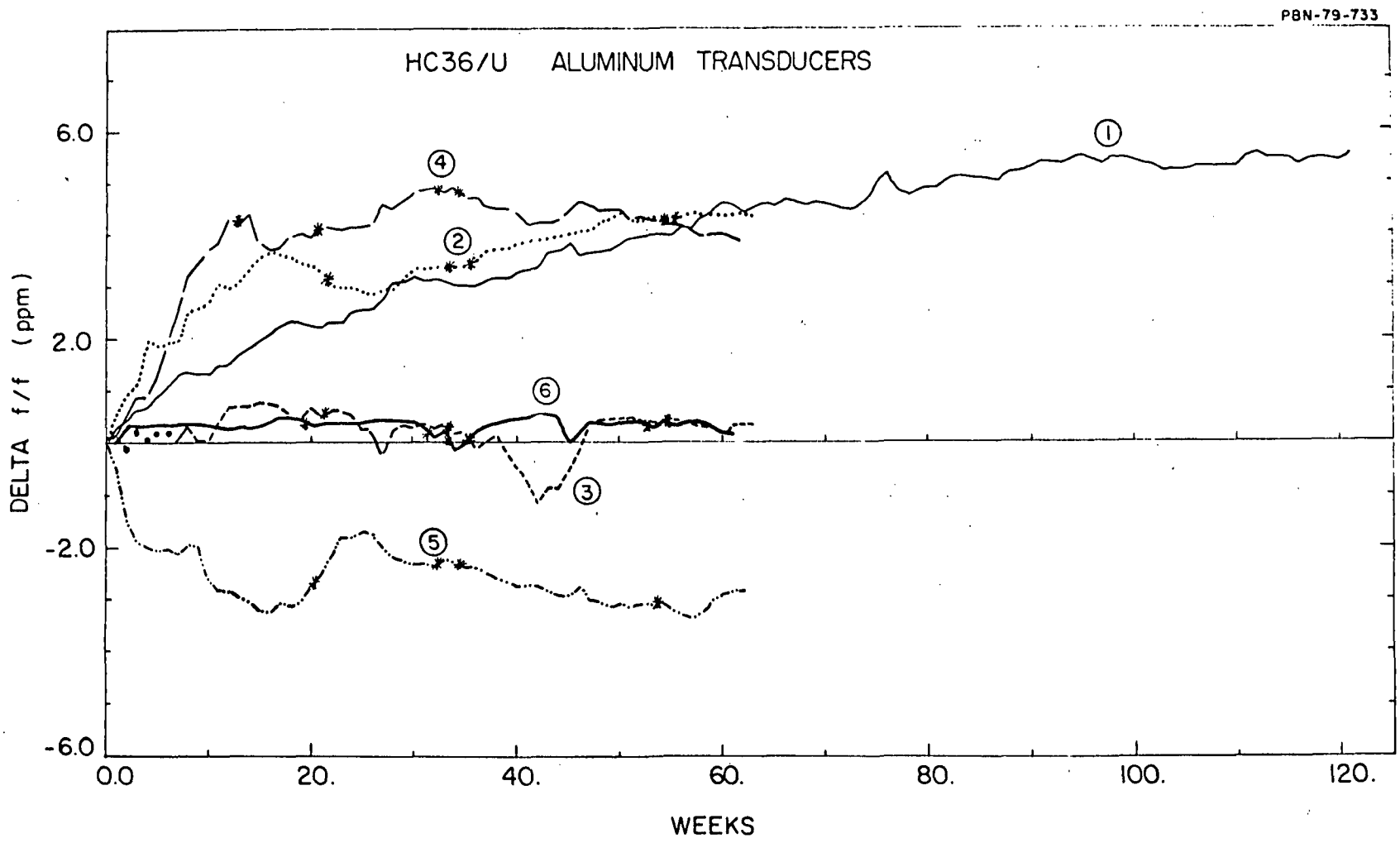

Figure 1. Aging Data for SAW Devices, with Aluminum Transducer, Sealed in HC36/u Enclosures. Asterisks (*) indicate the occurrence of power interruption.

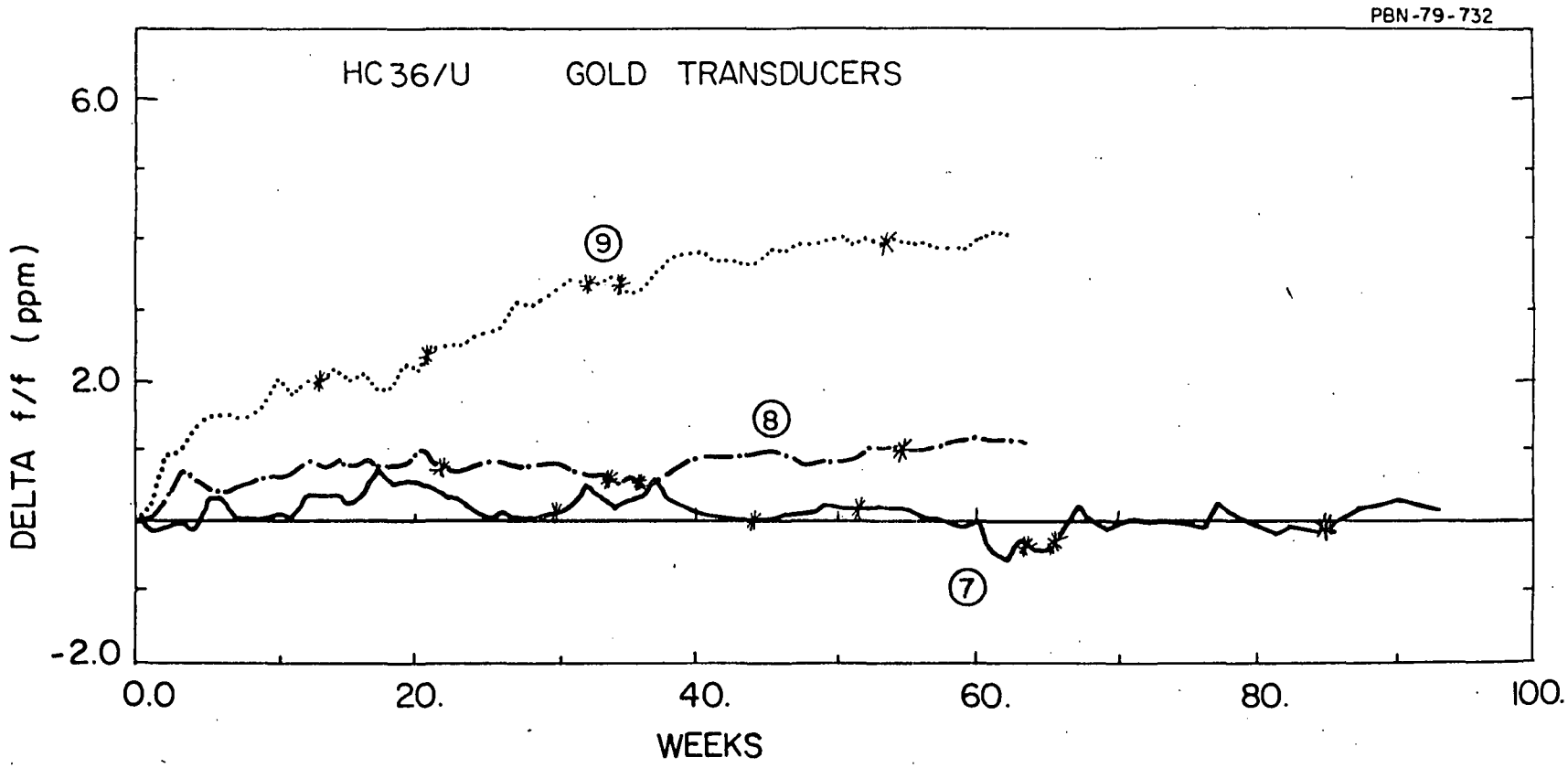

Figure 2. Aging Data for SAW Devices; with Gold Transducers, Sealed in HC36/u Enclosures.

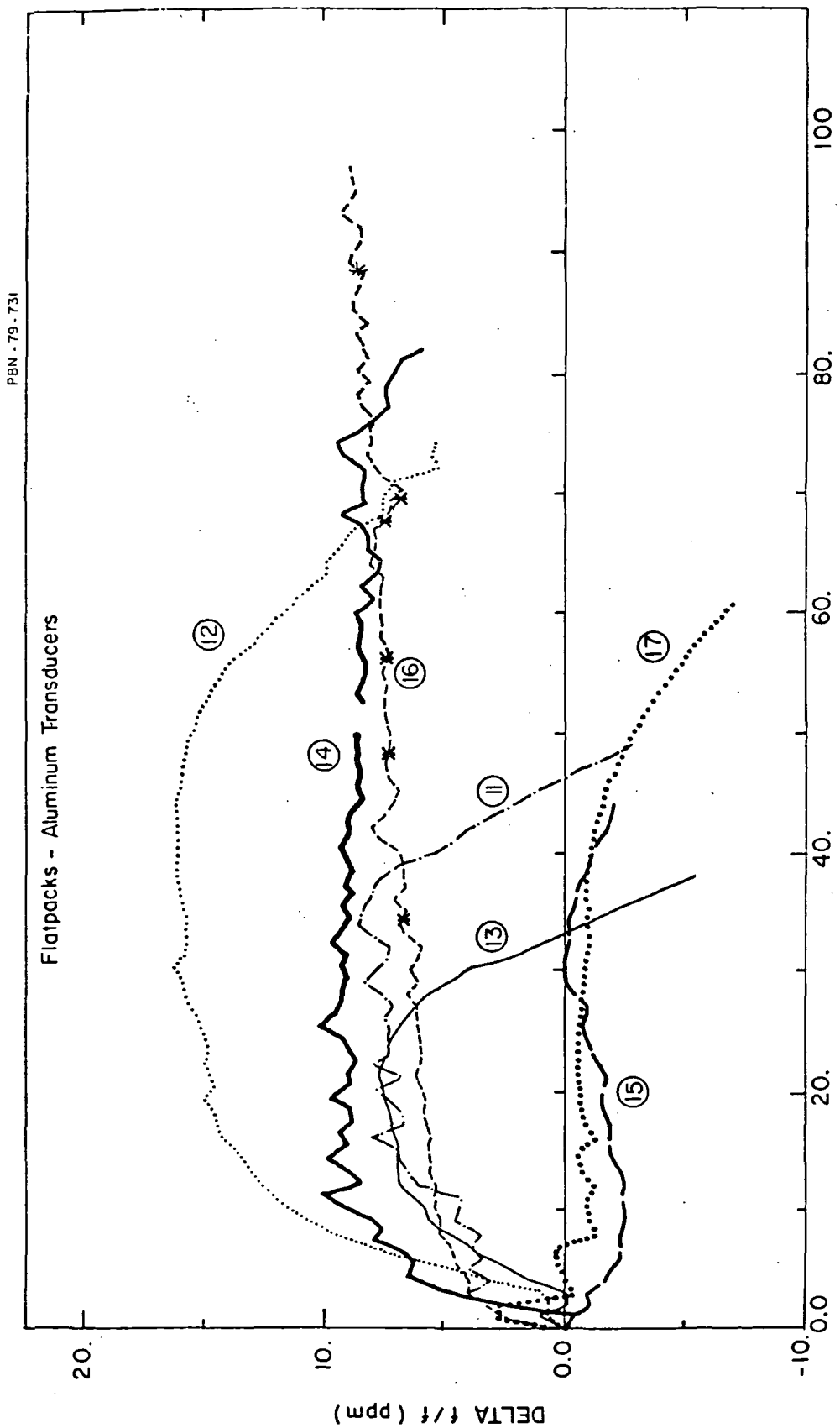

Figure 3. Aging Data for SAW Devices, with Aluminum Transducers, Sealed in Flatpacks.